CÉLIO HELDER RESENDE DE SOUSA

EVALUATING SEGMENTATION AND CLASSIFICATION APPROACHES USING RAPIDEYE DATA FOR VEGETATION MAPPING IN MINAS GERAIS, BRAZIL

LAVRAS – MG

2013

CÉLIO HELDER RESENDE DE SOUSA

EVALUATING SEGMENTATION AND CLASSIFICATION APPROACHES USING RAPIDEYE DATA FOR VEGETATION MAPPING IN MINAS GERAIS, BRAZIL

Dissertação apresentada à Universidade Federal de Lavras como parte das exigências do programa de Pós-Graduação Strictu Sensu em Engenharia Florestal, área de concentração em Manejo Florestal, para a obtenção do título de mestre.

Orientador

Dr. Luis Marcelo Tavares de Carvalho

LAVRAS – MG

2013

Ficha Catalográfica Elaborada pela Divisão de Processos Técnicos da Biblioteca da UFLA

Sousa, Célio Helder Resende de.
Evaluating segmentation and classification approaches using rapideye data for vegetation mapping in Minas Gerais, Brazil / Célio Helder Resende de Sousa. – Lavras : UFLA, 2013.
82 p. : il.

Dissertação (mestrado) – Universidade Federal de Lavras, 2013.
Orientador: Luis Marcelo Tavares de Carvalho.
Bibliografia.

1. Imagens de sensoriamento remoto. 2. Medidas de qualidade. 3. Objetos-referência. 4. Classes de cobertura do solo. 5. Algoritmos de aprendizagem. I. Universidade Federal de Lavras. II. Título.

CDD – 634.9285

CÉLIO HELDER RESENDE DE SOUSA

EVALUATING SEGMENTATION AND CLASSIFICATION APPROACHES USING RAPIDEYE DATA FOR VEGETATION MAPPING IN MINAS GERAIS, BRAZIL

Dissertação apresentada à Universidade Federal de Lavras como parte das exigências do programa de Pós-Graduação Stricto Sensu em Engenharia Florestal, área de concentração em Manejo Florestal, para a obtenção do título de mestre.

APROVADA em 28 de Fevereiro de 2013

Gilson Alexandre Ostward Pedro da Costa	PUC-Rio
Glaucia Miranda Ramirez	UFLA

Dr. Luis Marcelo Tavares de Carvalho

Orientador

LAVRAS – MG

2013

ACKNOWLEDGEMENTS

I am deeply grateful to God, for my life and wisdom. For the great opportunities, the wonders and the miracles that constantly fill my life. Thank you Lord!

Thanks to my dear mother who, throughout this journey, was at my side supporting me in the difficult moments and sharing my joys and achievements. Thank you!

Thanks to Prof. Dr. Luis Marcelo (a.k.a. Passarinho), who offered me the opportunity to work with him, for contributing to the definition of the subject of this dissertation and for providing invaluable scientific feedback that improved the quality of this research. Thanks Passarinho!

I wish to express my gratitude to Prof. Dr. Olaf Niemann for accepting me as a visiting research student for 5 months at the Department of Geography in the University of Victoria, Canada. Also, thanks to my colleagues Roger, Fabio, Diana, Geoff and Hei-Hei who provided a funny and productive work environment.

I would like to thank my dear friend and 'sister' Joyce (Jo, Joka, Joycinha) for the affection, friendship, companionship and complicity. Thanks for being present at all crucial moments of this journey. It has been 5 years of undergraduation and 2 years of master's sharing the joys and difficulties, always working together. Without you, all this would have been much harder. To you, my eternal admiration and friendship. Thanks for everything, my friend!

To my dear friends and no less precious: Matheus, André, Marcela and Aline. Each of you played a very important role in this achievement. Thanks Matheus, even in your absence, you advised me in my decisions with care and wisdom. You are our eternal leader. Thanks for always being by my side and vibrate for each achievement! I love you, man!

Marcela, thank you for understanding me in the worst, most complex and funny daydreams. Thank you for making this one of the most memorable period of my life. You're the best!

André, thanks for the moments of companionship. Only we know what we've been through… spending nights and weekends working (most of the time at the University). Also thank you very much for all the support during the Ph.D application process. If it weren't up to you, I don't know what I would've done. I deeply hope we can be colleagues during the Ph.D and I'm sure I'll dedicate you another whole paragraph in my thesis' acknowledgments. Thanks for everything, buddy!

Thank you Aline, that even from your distance, always supported me in (almost) everything. Thanks for your precious advices. Thanks for listening with your never-ending patience.

And finally, I would like to show my gratitude to Carol, Lisiane, Tássia and Polyanne: my dear friends and the best labmates in the world! Thank you, guys!

To my mother and my dear friends…

… A never-ending source of inspiration

CONTENTS

RESUMO

Este trabalho tem como objetivo principal investigar diferentes abordagens de segmentação e classificação de imagens de sensoriamento remoto para o mapeamento de áreas vegetadas no estado de Minas Gerais. Como ponto de partida, este trabalho foca no desenvolvimento de uma abordagem geral de seleção e avaliação da segmentação de imagens de alta resolução utilizando amostras de objetos reais, os quais são referidos como objetos-referencia. Uma série de medidas foi aplicada para a avaliação da qualidade da segmentação produzida por diferentes combinações de parâmetros em diferentes classes de cobertura do solo. Estas medidas foram utilizadas para gerar diferentes valores de ranking onde a combinação de parâmetros que obteve o maior ranking foi selecionada com a combinação ideal de parâmetros para a segmentação de uma determinada classe. Os resultados dessa abordagem mostraram que cada classe apresentou um parâmetro diferente de segmentação, o que reforça que uma abordagem de escala única pode não ser adequada para representar toda a área de estudo. Uma vez selecionado a melhor segmentação (produzida pelos parâmetros selecionados), foi aplicada uma abordagem de classificação baseada em diferentes classificadores: *Support Vector Machine*, Árvores de Decisão e *Random Forest*. O objetivo desta abordagem foi verificar o desempenho destes classificadores combinados à abordagem baseada em objetos em gerar mapas da cobertura do solo. Baseando-se nos resultados de comparação visual e de valores de exatidão, o mapa produzido pelo *Random Forest* retratou mais precisamente todas as classes de cobertura do solo do que os outros mapas produzidos pelo classificador Árvore de Decisão e *Support Vector Machine*.

Palavras-chave: Medidas de qualidade, objetos-referência, classes de cobertura do solo, algoritmos de aprendizagem.

ABSTRACT

This study aims to investigate different segmentation and classification approaches using remote sensing imagery for mapping vegetated areas in the state of Minas Gerais. As a starting point, this research focuses on developing a general approach for selecting and evaluating the segmentation of high-resolution images using samples of real objects, which are referred to as reference objects. Several goodness measures have been applied for the assessment of the quality of the segmentation produced by different combinations of parameters for different land-cover classes. These measurements were used to generate different ranking values where the combination of parameters that achieved the highest ranking was selected as the ideal combination of parameters for the segmentation of a given class. The results of this approach showed that each class had a different parameter as the best parameter, which reinforces that a single scale approach may not be adequate to represent the entire study area. Once selected the best segmentation (produced by selected parameters), we applied a classification approach based on different classifiers: Support Vector Machine, Decision Trees and Random Forest. The goal of this approach was to verify the performance of these classifiers combined with object-based approach to generate maps of land-cover classes. Based on the results of visual comparison and values of accuracy, the map produced by the Random Forest depicted more accurately all land-cover classes than the other maps produced by Decision Tree Classifier and Support Vector Machine.

Key-words: Goodness measures, reference objects, land-cover class, machine learning algorithms.

CHAPTER 1 - GENERAL INTRODUCTION

1 STRUCTURE OF THE DISSERTATION

This dissertation has been structured in two articles, according to the new available format from the Graduate Program in Forest Engineering formatting guidelines. The two articles were prepared according to the guidelines of the *International Journal of Remote Sensing*.

The content of each chapter is briefly summarized as follows:

Chapter 2 - Scale parameter selection for remote sensing image segmentation based on reference objects. This chapter focuses on the proposal of a procedure based on segmentation goodness measures for selecting optimal segmentation parameter values for remote sensing image segmentation. A supervised method based on manually delineated object was used. The methodological steps on selecting the reference objects, the goodness measures utilized and our selection procedure based on Global Score are presented. A single-class and a multi-class approach were analysed in order to verify whether is preferable a single or a multi-scale to represent the entire scene.

Chapter 3 - Object-based classification with selected machine learning algorithms for the classification of vegetated areas using high-resolution RapidEye imagery. In this chapter, the study focuses in an object-based image analysis approach for classifying land-cover classes over a vegetated landscape using three supervised machine learning algorithms. For the segmentation process, the optimal multi-class parameter value (400A - Chapter 2) was used. The methodological steps on selecting the object features, tuning the machine

learning algorithms parameters as well as the final classification maps are presented.

2 INTRODUCTION

In recent years, there has been an increasing interest in providing integration tools in the area of remote sensing for forest management. As it is already known, vegetation is a critical component of landscape and serves as an indicator of the overall ecosystem condition, environmental stress and landscape change at local, regional and global scales However, the perception of the difficulties in monitoring the earth's surface at regional and global scales led to the development of new operational solutions and, concomitantly, the development of new sensors.

Studies possible only by the use of airborne sensors can now be easily implemented with data from remote sensing with the advent of satellite sensors with high and very high spatial resolution. Among the various sensors available today, the RapidEye (which is the focus of this research), which produce images with 5 m spatial resolution, has proven suitable for studies in the context of vegetation since the satellites were designed to be used mainly to monitor agricultural and environmental resources (RAPIDEYE, 2011).

Hence, with the development of more advanced sensors, the level of detail within the images has increased considerably, allowing smaller features to be mapped on the Earth’s surface. However, new challenges have emerged when processing these images, resulting in a poor performance of traditional pixel-based approaches. The main challenges are related to the increased spatial heterogeneity and the reduced size of objects that can be detected. Consequently, concerns regarding the accuracy and fidelity of the derived products also increased.

In the last decade, a new approach has been extensively used to address these challenges: GEOBIA – Geographic Object-Based Image Analysis. According to GEOBIA, the basic unit of processing is no longer the pixel, but

objects composed of several pixels. There are several advantages in the application of a classification based on an object-based approach instead of pixel-based approach. Image objects, besides the spectral information, contain additional attributes (e.g. shape, texture, relational and contextual information) that can be used for classification purposes (BAATZ; SCHÄPE, 2000; BLASCHKE; STROBL, 2001). Moreover, segmentation produces homogeneous image objects, avoiding the induced salt-and-pepper effect (MEINEL; NEUBERT; REDER, 2001).

This new approach implied the prior segmentation of satellite images, which means grouping spectrally similar pixels in a single object according to a stop-threshold called ‘scale parameter’. However, the quality of the segmentation is closely related to the scale parameter used. Until now, no general approach for selecting this threshold exists.

There have been several significant advances in image segmentation process in the past few years. However, compared to the segmentation process itself, relatively little attention has been given to the evaluation of the segmentation results as well as to the development of a general approach to avoid the subjectivity in selecting a scale parameter. Since the quality of segmentation is closely related to the scale parameter used in the segmentation process, one of the major obstacles of object-based approach is to define an appropriate scale parameter for a specific type of image and object under investigation. The selection of the scale parameter is, mostly, based in the user experience or in a visual assessment of the image. Both cases are based human perception which is very difficult, time-consuming, subjective and the results may vary according to the user. In addition, the evaluation of the segmentation results is not yet a standard practice when conducting an object-based approach classification. In many cases, evaluation of segmentation is performed only

visually and taking into consideration the class or phenomenon under study which is also subjective.

Hence, one of the motivations in conducting this research is to avoid this undesired subjectivity by developing a general approach to evaluate and compare the results of segmentations performed by several parameter combinations and, based on the results, to select the best segmentation parameter.

The very next step in this process – which is also the next step of this research – is to conduct the classification based on the objects produced by the segmentation process. A classification is needed not only for a better understanding of the structure and composition of the resources and features under investigation, but also for the pattern recognition and for mapping areas in the earth's surface which presents the same meaning in the digital images. It is also known that a poor segmentation can strongly affect the overall accuracy of the classification. It is essential, however, to be able to determine whether inaccuracy in the classification process is due to a poor classifier or a poor segmentation, or even both. Thus, the first step of the analysis must be to avoid the influence of a poor segmentation in the overall accuracy by choosing the best set of parameters to produce good segmentation results.

In this context, a number of studies have been testing different classifiers in order to verify their influence in the final overall accuracy. Over the last years, machine learning algorithms have shown great potential to deal with a high number of predictors from the object-based approach as well as to improve the accuracy and reliability of remote sensing image classification. Machine learning algorithms have been intensively used for classification purposes in remote sensing showing improvements in classification accuracy.

For this reason, the second part of this research focuses in evaluating their robustness in conducting classifications in an area with wide variety of

environmental settings due the different land-cover classes in order to obtain good classification results and, consequently, reliable information about the entire area.

3 Research objectives

In order to help bridge the current research gap that exists, this dissertation has the following objectives:

- To develop a procedure based on segmentation goodness measures and reference objects for selecting the appropriate image segmentation parameter values from a set of potential combinations produced by the Multi-Resolution Segmentation (MRS);
- To assess the performance of different goodness measures in choosing an "optimal" from a large set of candidate segmentations produced by a set of different parameter values;
- After the selection of the optimal segmentation parameter value, to examine the object-based approach in conducting classifications of a vegetated area in RapidEye data with a selection of machine learning algorithms such as Decision Trees, Random Forest and Support Vector Machines.
- To produce a step-by-step tutorial on how to use these machine learning algorithms in the R environment for future studies.

4 BACKGROUND

This section aims to provide the required theoretical fundaments for this research.

4.1 Remote Sensing

According to many definitions of the term ‘Remote Sensing’ found in literature (MORAES, 2002; LILLESAND; KIEFER, 2000; RICHARD; JYA, 2006; DE JONG; MEER, 2004; SCHOWENGERDT, 2007) a broad definition can be stated as:

> *The science and art of obtaining information about an object, area or phenomenon in the Earth’s surface through the detection, acquisition and analysis (the information interpretation and extraction) of the electromagnetic energy emitted or reflected by terrestrial objects and recorded by a device that is not in direct contact with the object, area, or phenomenon under investigation.*

Remote sensing, also called ‘*Earth Observation*’, refers in a general sense to the instrumentation, techniques and methods used to observe, or sense, the surface of the earth, usually by the formation of an image in a position, stationary or mobile, at a certain distance remote from that surface (BUITEN; CLEVERS, 1994).

Concerning the mentioned concept, remote sensing researchers, technology producers, ecologists, forest and land managers agree in the potential role of remote sensing as an information resource to support sustainable forest management. This potential is based largely on the unique characteristics that

remote sensing data provides: synoptic, repetitive, quantitative, and spatial explicit capabilities (FRANKLING, 2001).

4.1.1 Electromagnetic Spectrum

The electromagnetic spectrum is a set of waves of electromagnetic radiation that differ by the value of their frequency and length. These waves are then classified into distinct regions (Figure 1). This radiation - which is defined according to Moraes (2002) as a form of energy which propagates without the need of a media, as waves or electromagnetic particles - is used in obtaining data from remote sensing and it is represented continuously in terms of wavelength, frequency or energy (MORAES, 2002; ROSENDO, 2005).

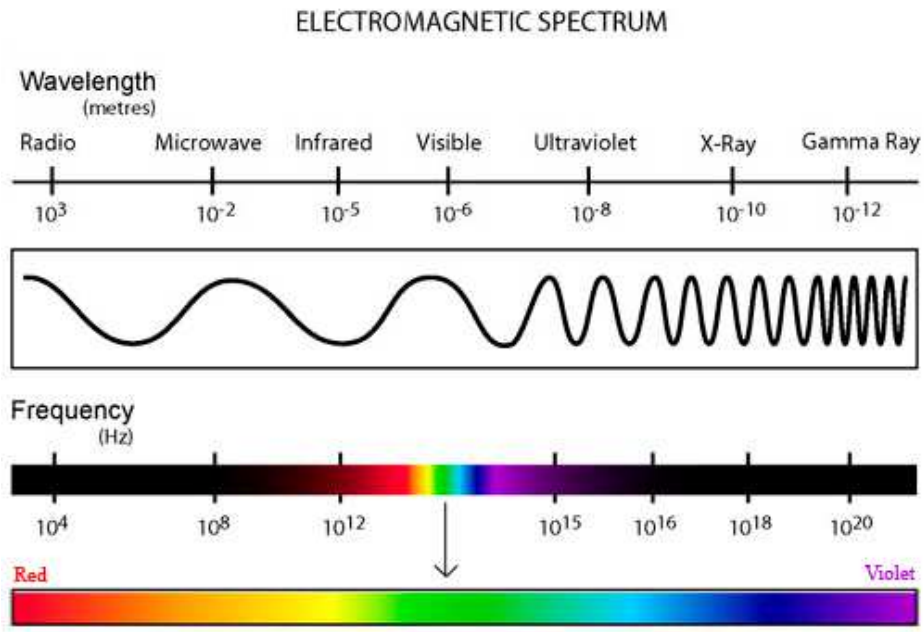

Figure 1 The Electromagnetic Spectrum

The segments of the electromagnetic spectrum used by remote sensing are the visible and infrared spectrum (ROSENDO, 2005). The visible spectrum is the region of the spectrum which is perceived by the human eye and covers colors from violet to red. The infrared is divided into three: near-infrared (0.7 to 1.3 μM), mid-infrared (1.3 to 6.0 μm) and thermal infrared (6.0 to 1000 μM) (Table 1). The ranges that include the set of frequencies or length waves of the electromagnetic spectrum are called *spectral bands*.

Tabel 1 Regions of the electromagnetic spectrum and their wavelength ranges

Regions		**Wavelength**
Gamma Ray		< 0,003 – 0,4 μm
X Ray		0,03 – 3,0 nm
Ultraviolet		0,003 – 0,4 μm
	Blue	0,45 – 0,50 μm
Visible	Green	0,50 – 0,54 μm
	Red	0,65 – 0,72 μm
Near Infrared		0,72 – 1,3 μm
Mid Infrared		1,3 – 4,0 μm
Far Infrared		4,0 – 300 μm
Microwaves		1,0 – 100 cm
Radio		> 100 cm

The sun and the Earth are the two main natural sources of electromagnetic energy used in remote sensing of land surface (MORAES, 2002). Regardless of its source, all the radiation passes through the atmosphere. However, the length traveled through the atmospheric layers can vary widely. Thus, the effect of the atmosphere in the sensing may vary depending on the variations in length traveled by the radiation, the atmospheric conditions in the moment and of the wavelengths involved in the process (LILLESAND; KIEFER, 2000).

The solar radiation that focus on earth's surface is, in parts, scattered or reflected by particles in the atmosphere. Part of the radiation that hits the target is reflected or emitted. The phenomenon related to the portion of energy which

is reflected is called *Reflectance* (ρ) and it is important to remote sensing since the orbital sensors registers the reflectance from the objects in Earth's surface. Each object in Earth's surface which emits or reflects radiation has a spectral fit for each wavelength of the electromagnetic spectrum.

4.2 RapidEye

Known as RapidEye, the multispectral satellite constellation was designed by MacDonald Dettwiler and Associates (MDA) of Richmond, Canada and launched into space on August 29, 2008 (RAPIDEYE, 2011). The system is run by a private provider of geospatial information and services known as German RapidEye AG (BECKETT; ROBERTSON; STEYN, 2010).

The system consists of five identical satellites 150 kg equally spaced around the orbit (TCY et al., 2005). The satellites operate in an orbit at 630 km altitude, each with a pubshbroom sensor, five multispectral bands and spatial resolution of 6.5 meters. The system is able to access any point on the surface of the Earth daily between latitudes -84º to +84º (RAPIDEYE, 2011; BECKETT; ROBERTSON; STEYN, 2010).

The RapidEye products are available in two processing levels: 1B and 3A. The products that receive a Level 1B radiometric correction have a correction of the sensor, and receive data from the satellite altitude; On the other hand, 3A products receive radiometric, geometric and sensor correction (RAPIDEYE, 2011). Also, the RapidEye images have the Red Edge band (690-730 nm), specific for monitoring the photosynthetic activity of the vegetation. Conducting a study to evaluate the contribution of RedEdge band in land use classification, Schuster, Förster and Kleinschmit (2012) calculated 24 spectral indices in which the Red Edge band was incorporated. Among the indices tested, was the NDVI (Normalized Difference Vegetation Index) with adaptations for the Red Edge.

The authors used the machine learning algorithms such as Support Vector Machine and Maximum Likelihood to conduct the classifications and as a result, found that for both, there was a slight improvement in the overall accuracy of the classification when they introduced the band Red Edge and indexes as inputs for classification.

4.3 Image segmentation and object-based image classification

The availability of high spatial resolution images obtained from satellites and airborne sensors has increased in recent years. However, traditional methods for classification based on pixels are not suitable for these types of images. For Yu et al. (2006) this is due to the fact that a single pixel usually represents only a small part of the target object classification in images with high spatial resolution. When the classification is done, the high degrees of spectral variability found in classes, such as shadows caused by differences in the canopy, etc. reduce the separability between classes, resulting in low classification accuracy. Moreover, the unsatisfactory results of this approach can be attributed to the fact that contextual and geometric information of the image are highly neglected.

An alternative approach to the traditional pixel-based approach is the object-oriented approach (HAY; CASTILLA, 2008). The basic idea of this process is the grouping adjacent pixels into objects spectrally homogenous and thereby lead to the classification of the objects as being the minimum unit of image processing (YU et al., 2006). Using these objects as basic units of analysis has many benefits, such as reducing spectral variability within the class and the ability to include spatial and contextual information such as size, shape, texture and topological relations (BENZ et al., 2004). The objects are created through the segmentation and it can be defined as the process of partitioning an

image into non-overlapping regions. This process requires previous image segmentation for object delineation through a stop threshold called ‘scale parameter’. However, no general approach for selecting this parameter exists.

The classification is the very next step in this approach. Several studies have been studies testing different classifiers such as machine learning algorithms in order to verify their influence in the final overall accuracy. These new classifiers have shown great potential in conducting classifications and improve the accuracy of the final classification (HUANG; DAVIS; TOWNSHEND, 2002; PAL, 2005; HAM et al., 2005; GISLASON; BENEDIKTSSON; SVEINSSON, 2006; LALIBERTE et al., 2006; LAWRENCE; WOOD; SHELEY, 2006; YAN et al. 2006; CHAN; PAELINCKX, 2008; PLATT; RAPOZA, 2008; WATTS et al., 2009; OTUKEI; BLASCHKE, 2010; STUMPF; KERLE, 2011; MYINT et al., 2011; DURO; FRANKLIN; DUBÉ, 2012).

References

BAATZ, M.; SCHÄPE, A. Multiresolution segmentation – an optimization approach for high quality multi-scale image segmentation. In: STROBL. BLASCHKE. GRIESEBNER (Ed.). **Angewandte Geographische Informations verarbeitung XII**. Heidelberg: Wichmann-Verlag, 2000. p. 12-23.

BLASCHKE, T.; STROBL, J. What is wrong with pixels? Some recent developments interfacing remote sensing and GIS. **GISZeitschrift für Geoinformationssysteme**, v. 6, p. 12-17, 2001.

BECKETT, K.; ROBERTSON, B.; STEYN, J. MTF Characterization and Deconvolution of RapidEye Imagery. In: GEOSCIENCE AND REMOTE SENSING SYMPOSIUM, 2010. Richmond: IEEE International, 2010. p. 3390-3393. Disponível em: <http://ieeexplore.ieee.org/xpl/login.jsp?tp=&arnumber=5650362&url=http%3A%2F%2Fieeexplore.ieee.org%2Fxpls%2Fabs_all.jsp%3Farnumber%3D5650362 >. Acesso em: 10 dez. 2012

BENZ, U. C. et al. Multiresolution, object-oriented fuzzy analysis of remote sensing data for GIS-ready information. **ISPRS Journal of Photogrammetry and Remote Sensing**, v. 58, p. 239–258, 2004.

BUITEN, H. J.; CLEVERS, G. P. W. **Land observation by remote sensing**: theory and applications. Yverdon, Switzerland: Taylor & Francis, 1994. 642 p.

CHAN, J. C.-W.; PAELINCKX, D. Evaluation of Random Forest and Adaboost tree-based ensemble classification and spectral band selection for ecotope mapping using airborne hyperspectral imagery. **Remote Sensing of Environment,** v. 112, p. 2999–3011, 2008.

DE JONG, S. M.; MEER, F. D. van der. **Remote sensing image analysis**: including the spatial domain. Dordrecht: Kluwer Academic, 2004. v. 5.

DURO, D. C.; FRANKLIN, S. E.; DUBÉ, M. G. A comparison of pixel-based and object-based image analysis with selected machine learning algorithms for the classification of agricultural landscapes using SPOT-5 HRG imagery. **Remote Sensing of Environment,** v. 118, p. 259–272, 2012.

FRANKLIN, S. E. **remote sensing for sustainable forest management**. Boca Raton: Lewis, 2001. 458 p.

GISLASON, P. O.; BENEDIKTSSON, J. A.; SVEINSSON, J. R. Random forest classification of multisource remote sensing and geographic data. In: IEEE INTERNATIONAL GEOSCIENCE AND REMOTE SENSING SYMPOSIUM, 4., 2004. **Proceedings**… IEEE, 2004. p. 1049–1052.

HAM, J. et al. Investigation of the *Random Forest* framework for classification of hyperspectraldata. **IEEE Transactions on Geoscience and Remote Sensing**, v. 43, p. 492−501, 2005.

HAY, G. J.; CASTILLA, G. Geographic Object-based Image Analysis (GEOBIA): a new name for a new discipline. In: BLASCHKE T.; LANG, S.; HAY, G. J. (Ed.). **Object-based image analysis**: spatial concepts for knowledge-driven remote sensing applications. Berlin: Springer-Verlag, 2008.

HUANG, C.; DAVIS, L. S.; TOWNSHEND, J. R. G. An assessment of support vector machines for land cover classification. **International Journal of Remote Sensing**, v. 23, p. 725–749, 2002.

LALIBERTE, A. S. et al. Object-oriented image analysis for mapping shrub encroachment from 1937 to 2003 in southern New Mexico. **Remote Sensing of Environment**, v. 93, p. 198–210, 2004.

LAWRENCE, R. L.; WOOD, S. D.; SHELEY, R. L. Mapping invasive plants using hyperspectral imagery and Breiman Cutler classifications (randomForest). **Remote Sensing of Environment**, v. 100, p. 356–362, 2006.

LILLESAND, T. M.; KIEFER, R. W. **Remote sensing and image interpretation**. 4. ed. New York: J. Wiley, 2000. 721 p.

MEINEL, G.; NEUBERT, M.; REDER, J. Pixelorientierte versus segmentorientierte Klassification von IKONOS-Satellitenbilddaten: ein Methodenvergleich (Pixel- oriented versus segment-oriented classification of IKONOS satellite image data: comparison of methods). **Photogrammetrie-Fernerkundung-Geoinformation,** v. 3, p. 157-160, 2001.

MORAES, E. C. Sensoriamento remoto no estudo da vegetação: diagnosticando a Mata Atlântica. In: INSTITUTO NACIONAL DE PESQUISAS ESPACIAIS. **Curso de uso do sensoriamento remoto no estudo do meio ambiente**. São José dos Campos, 2002. Cap.1.

MYINT, S. W. et al. Per-pixel vs. object-based classification of urban land cover extraction using high spatial resolution imagery. **Remote Sensing of Environment**, v. 115, p. 1145–1161, 2011.

OTUKEI, J. R.; BLASCHKE, T. Land cover change assessment using decision trees, support vector machines and maximum likelihood classification algorithms. **International Journal of Applied Earth Observation and Geoinformation**, v. 12, p. S27–S31, 2010.

PAL, M. Random forest classifier for remote sensing classification. **International Journal of Remote Sensing**, v. 26, p. 217–222, 2005.

PLATT, R. V.; RAPOZA, L. An evaluation of an object-oriented paradigm for land use/land cover classification. **The Professional Geographer**, v. 60, p. 87–100, 2008.

RAPIDEYE, A. G. **RapidEye Standard Image Specifications**.Version 3.2. May 2011. Disponível em: <http://www.rapideye.de/upload/RE_Product_Specifications_ENG.pdf>. Acesso em: 10 dez. 2012.

RICHARDS, J. A.; JIA, X. **Remote sensing digital image analysis** – an introduction. 4. ed. Berlin: Springer-Verlag Berlin Heidelberg. 2006. 454 p.

ROSENDO, J. S. R. **Índices de vegetação e monitoramento do uso do solo e cobertura vegetal na bacia do Rio Araguari – MG – utilizando dados do sensor MODIS.** 2005. 130 p. Dissertação (Mestrado em Geografia)-Universidade Federal de Uberlândia, Uberlândia, 2005.

SCHOWENGERDT, R. A. **Remote Sensing**: models and methods for Image processing. 3. ed. New York: Elselvier, 2007. 558 p.

SCHUSTER, C.; FÖRSTER, M.; KLEINSCHMIT, B. Testing the red edge channel for improving land-use classifications based on high-resolution multi-spectral satellite data. **International Journal of Remote Sensing**, v. 33, p. 5583–5599, 2012

STUMPF, A.; KERLE, N. Object-oriented mapping of landslides using Random Forests. **Remote Sensing of Environment**, v. 115, p. 2564–2577, 2011.

TYC, G. et al. The RapidEye mission design. **ActaAstronautica,** v. 56, p. 213-219, 2005.

WATTS, J. D. et al. Monitoring of cropland practices for carbon sequestration purposes in north central Montana by Landsat remote sensing**. Remote Sensing of Environment**, v. 113, p. 1843–1852, 2009.

YAN, G. et al. Comparison of pixel-based and object-oriented image classification approaches—a case study in a coal fire area, Wuda, Inner Mongolia, China. **International Journal of Remote Sensing**, v. 27, p. 4039–4055, 2006.

YU, Q. et al. Object-based detailed vegetation classification with airborne high spatial resolution remote sensing imagery. **Photogrammetric Engineering & Remote Sensing**, v. 72, p. 799–811, 2006.

CHAPER 2

(Prepared according to International Journal of Remote Sensing guidelines)

SCALE PARAMETER SELECTION FOR REMOTE SENSING IMAGE SEGMENTATION BASED ON REFERENCE OBJECTS

C.H.R. de Sousa[†], L.M.T. de Carvalho[†] and K.O. Niemann[‡]

[†]*Department of Forest Sciences, Federal University of Lavras, Lavras, Brazil*

[‡]*Department of Geography, University of Victoria, Victoria, British Columbia, Canada*

[†]Universidade Federal de Lavras, Departamento de Ciências Florestais, Campus Universitário, Caixa Postal 3037, CEP 37200-000, Lavras, MG – Brasil

[‡]University of Victoria, Department of Geography, Social Sciences & Mathematics Bldg, Rm B203, 3800 Finnerty Road, Victoria, BC, Canada V8P 5C2

Corresponding author. E-mail: celiohelder@gmail.com

Abstract: This paper presents a procedure based on measures of segmentation goodness and on reference objects for selecting appropriate segmentation parameter values from a set of potential combinations. For this study, we used a 5m spatial resolution RapidEye image. A set of 20 reference objects and 15 test objects were manually delineated. For evaluating segmentation results, we used quality measures designed to compare the results of object-based image segmentation with sets of training objects extracted from the image of interest. These quality measures are mostly related to over-segmentation and under-segmentation problems. We computed a score for each segmentation parameter according to the value obtained in each measures. The results show that the measures have different performance in terms of the identification of which parameter combination is better. However, based on the visual assessment of the

test objects, the proposed procedure showed to be efficient in identifying a suitable scale parameter value for each class. The results also reinforced the statement that a single-scale approach is not adequate for representing all classes as some of them may be under or over-segmented using a single scale parameter.
Keywords: parameters selection, quality measures

1. Introduction

Classification of remotely sensed images for mapping and monitoring land cover had fundamental importance in recent decades, in particular, due to the development of new techniques and computer programs that enhanced the analysis and manipulation of increasingly available digital data. The classification process can be divided into two general approaches: i) pixel-based, and ii) object-based. The former has been traditionally used since the early stages of remote sensing image processing, while the latter has become more common in recent years (Blaschke 2010), after the availability of higher spatial resolution imagery.

Also according to Blaschke (2010), there is a consensus in the field of remote sensing that some of the unsatisfactory results in classification of high spatial resolution images using pixel-based methods can be attributed to the fact that both geometrical and contextual information contained in the images are ignored. To address these issues, object-based analysis has become a concept widely used in geoscience studies to explore the geometric and contextual information from image data.

Object-based methods require previous image segmentation for object delineation. Therefore, many segmentation algorithms have been developed aiming at the extraction of meaningful image objects. In most algorithms, users need to set one or more parameters that affect the average size and the number of objects generated during segmentation. However, parameter selection is uncertain. A specific set of parameters may produce a good segmentation result

when considering a homogeneous scene but this is not valid when a heterogeneous scene is under consideration. Since the landscape mostly consist of different types of environmental settings and varies in size (e.g. trees, rivers, forest remnants, etc.), a single-scale approach might not be appropriate as some features within the scene will be under-segmented (when part of the feature become part of another feature) or over-segmented (when the feature is segmented into smaller objects).

Since the effectiveness of the object-based approach is directly affected by the segmentation quality, studies that deal with evaluation of image segmentation have become an emergent topic in remote sensing.

Zhang (1996) categorized the evaluation methods into three types: analytical, empirical goodness and empirical discrepancy methods. The analytical methods evaluate the segmentation algorithm itself, considering its principles, requirements, utilities and complexity, etc., and the information provided by these methods are qualitative. However, in certain cases, these methods can provide quantitative information about the algorithms. Empirical quality methods as well as the analytical methods are also referred to as *unsupervised methods* of evaluation. These methods evaluate the performance of algorithms through quality measures such as, for example, statistical measures of pixels and the shape of objects, without the need for a reference or prior knowledge of the segmentation considered correct. On the other hand, the empirical discrepancy methods involve comparing multiple image segmentations with a manually delineated image object, also referred to as references, thus classified as *supervised methods*.

There are some studies that have used unsupervised methods of evaluation (Espindola et al. 2006; Chabrier et al. 2006; Kim, Madden and Warner, 2008). A detailed description of unsupervised methods can be found in

Zhang, Fritts and Goldman (2008). However, according to Zhang, Xiao and Feng (2012) the supervised methods are the most used.

Several studies have applied supervised methods using different quality measures. Some of them have used indices such as *Area Fit Index* (Lucieer and Stein 2002), *Spatial Overlap Index* (Zou et al. 2004) and the *Quality Rate* (Weidner 2008) for quantifying the goodness of the segmentation. Others have tried to use measures based on shape such as *area* and *perimeter* (Neubert and Meinel 2003), *circularity* (Yang et al. 1995) and *shape index* (Neubert and Meinel 2003) unlike Cardoso and Corte-Real (2005), Jiang et al. (2006) and Gavet and Pinoli (2011) which have used distance functions on the evaluation procedures. On the other hand, Clinton et al. (2010) has used combined measures whereas Ramón et al. (2001) has presented a hybrid measure based on empirical goodness and empirical discrepancy methods.

Despite many studies that assess the quality of the segmentation process, there are few that provide subsidies for choosing the optimal scale parameter based on the evaluation of quality measures. Thus, the purpose of this study is to present a parameter selection procedure based on measures of segmentation goodness for selecting the appropriate scale parameter value from a set of potential combinations.

2. Methods

2.1. Data and study area

A high spatial resolution RapidEye image from the southern region of Minas Gerais, Brazil, was used (Figure 1). RapidEye imagery presents 5,0 m spatial resolution with five channels: blue (0,44 – 0,51 μm), green (0,52 – 0,59 μm), red (0,6, – 0,68 μm), red edge (0,69 – 0,73 μm) and near infra-red (0,76 –

0,85 μm) and a radiometric resolution of 12 bit. This data set was acquired at standard processing level (orthorectified) by Minas Gerais state government in June, 2010.

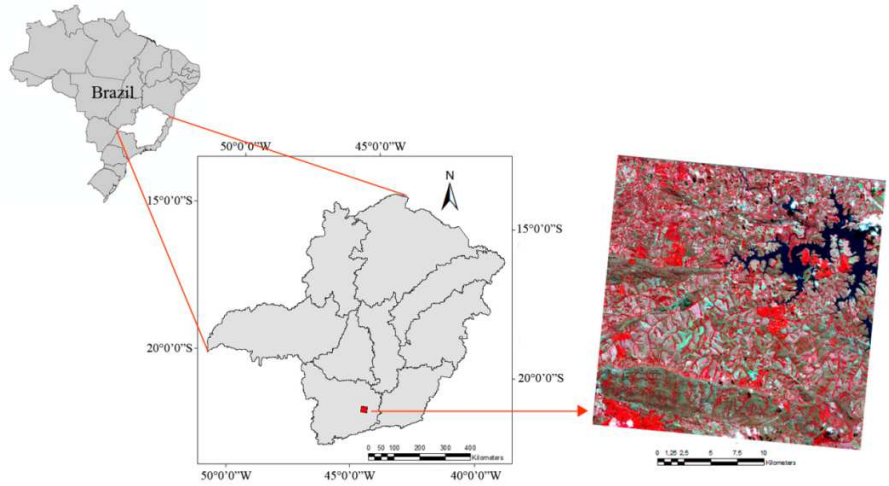

Figure 1. Study area located in Minas Gerais. Brazil.

This image has an area of 77 x 77 km over the municipalities of São Vicente de Minas, Minduri, Cruzília, Luminárias and Carrancas. The area is part of the Rio Grande basin, called Campo das Vertentes. The main types of native vegetation are savannah, seasonal forest, rocky field and gallery forest. The area is located within the transition between two major Brazilian Biomes. The Atlantic Rainforest is one of the most important Biomes in the country and originally covered about 1 million square kilometers within 17 states, representing 16% of the country area (Galindo-Leal and Câmara 2003). However, forested areas within this Biome have been decreasing since the colonial period due to agricultural cycles and to the expansion of cultivated fields. Nowadays, forests cover approximately 98000 square kilometers (8% of the original cover) and are still under strong anthropogenic pressure. The land-

cover in the study area basically includes remnants of native grassland, rocky fields, savannah and forest, as well as open water, pasture, eucalyptus, and crops.

2.2. Image segmentation

Image segmentation represents the first step in object-based image analysis. Many segmentation algorithms have been developed in recent years and all of them aim at deriving homogeneous image segments. The multi-resolution image segmentation (MRS) implemented in eCognition Developer® software is a frequently used algorithm in Earth sciences (Blaschke 2010). The MRS algorithm uses a "bottom-up" region neighboring objects based on a set of user-defined parameters such as scale, color/shape, and smoothness/compactness defining a "stopping threshold". Additional information regarding the segmentation algorithm can be found in Benz et al. (2004).

For this study, image segmentation was performed using 9 different scale parameters values ranging from 100 to 1000 (100, 150, 200, 250, 300, 400, 500, 750 and 1000) using the MRS. Thus, the segmentation and further evaluation measures could be analysed at various scales. For each scale parameter, a set of three combinations of color/shape values was used, comprising 27 scale+color/shape combinations. The smoothness/compactness value were held constant (0.5). The values of color/shape used were 0.1, 0.3 and 0.5 thereafter mentioned as A, B and C, respectively. All of the segmented images were then exported as polygon shape files for further analysis in ArcGIS 9.8

2.3. Measures of segmentation goodness

2.3.1. Reference digitization

According to the available literature, there are a large number of segmentation evaluation methods. We focused particularly on the supervised methods in which a set of manually delineated objects will be used as reference to compare to the segmentation results.

All reference objects used in this study were well segmented since their boundaries are very sharp. Therefore, we relied on our past experience with the study area as well as conducting object-based classifications in these land-cover classes to guide the selection of reference objects.

In this study, 20 reference objects from five land-cover classes - Bareland, Eucalyptus, Grassland, Forest remnants and Pasture - were manually delineated using ENVI 4.8 (Figure 2). For each class, we carefully selected the objects varying in shape, size and location.

Figure 2. Representation of the 20 manually delineated reference objects from the five different land-cover classes. From the top left: Bareland, Eucalyptus, Grassland, Forest remnants and Pasture marked in red, light blue, green, white and blue respectively.

For the purpose of comparison, we also delineated 15 objects – thereafter referred as ‘test objects’ – in order to verify the segmentation results produced by the optimal scale parameter value presented by the proposed procedure based on the reference objects (Figure 3).

Figure 3. Representation of the 15 manually delineated test objects from the five different land-cover classes. From the top left: Bareland, Eucalyptus, Grassland, Forest remnants and Pasture marked in yellow, white, light blue, black and maroon, respectively.

2.3.2.Segmentation Evaluation Criteria

Since under-segmentation and over-segmentation are important issues for GEOBIA, the criteria for segmentation evaluation used in this study are mainly based on goodness measures, which give an indication of under-segmentation and over-segmentation.

We computed various goodness measures for each combination of segmentation parameters and different reference object sets (Bareland, Eucalyptus, Grassland, Forest remnants and Pasture).

For the purposes of describing the goodness measures used in this study, let us consider $X = \{x_i: i = 1…n\}$ as the set of n training objects, where $n = 20$; and $Y = \{y_j: j = 1…m\}$ as the set of m objects from the results of different segmentations (Figure 4a).

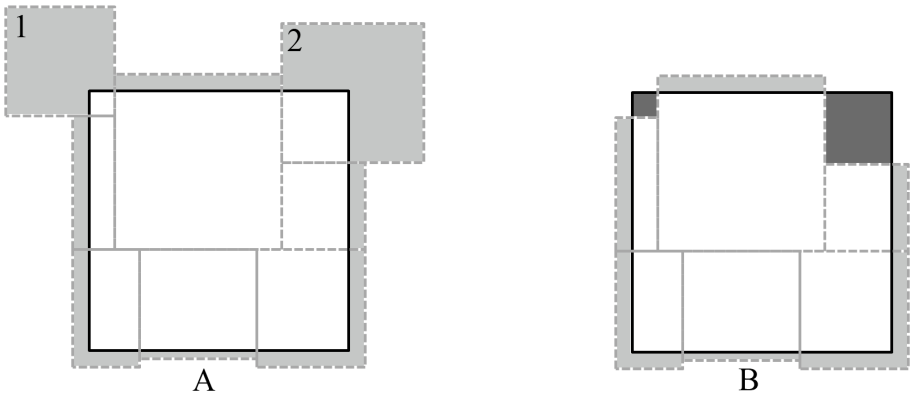

Figure 4. Schematic representation of the objects (dashed gray line) overlapping the reference object (solid black line). (A) The *Y* set indicating all the objects overlapping the reference object, including those with more than 25% of extra pixels (in light gray) (1 and 2). and; (B) the Y_a subset indicating the relevant objects within the reference and the lost areas (dark gray) due the exclusion of the objects 1 and 2.

Therefore, let us consider the Elementary Set Theory to describe $area(x_i \cap y_j)$ as the area of intersection of the training object x_i with the objects y_j; and $area(x_i \cup y_j)$ as the union of the area from the training object x_i with the objects y_j. In this study, our evaluation was performed only in the objects y_j which are relevant to the training object x_i, according to the following rule:

- $Y_a = y_j$: $area(x_i \cap y_j) / area(y_j) > 0{,}75$.

This rule will ensure that Y_a will contain only objects with more than 75% of its area within the reference object. In other words, objects with more than 25% of extra pixels may not properly represent the reference. This is an

indication of under-segmentation, which is not desired. The exclusion of these objects causes a loss of area, which is also an indication of under-segmentation (Figure 4b).

Möller et al. (2007) proposed the *Relative Area* (*RA*) metric:

$$RA = \frac{area(x_i \cap y_j)}{area(y_j)}, y_j \in Y \quad (1)$$

According to Möller et al. (2007), $RA \in [0,1]$ with 1 being an ideal segmentation.

Weidner (2008) proposed the Quality Rate (*QR*) index:

$$QR = 1 - \frac{area(x_i \cap y_j)}{area(x_i \cup y_j)}, y_j \in Y_a \quad (2)$$

Where, $QR \in [0,1]$ with 0 being an ideal segmentation.

Clinton et al. (2010) evaluated a modification of the *RA* metrics and both metrics were combined via Root Mean Square:

$$Oversegmentation = 1 - \frac{area(x_i \cap y_j)}{area(x_i)}, y_j \in Y_a \quad (3)$$

$$Undersegmentation = 1 - \frac{area(x_i \cap y_j)}{area(y_j)}, y_j \in Y_a \quad (4)$$

$$RMS = \sqrt{\frac{Oversegmentation^2 + Undersegmentation^2}{2}} \quad (5)$$

Both metrics are within the interval [0,1], with 0 being ideal. According to the authors, these modifications were made to compare with the original *RA* measure and to evaluate the measures over the relevant objects for each reference. These modifications are suitable for this study as we are evaluating the measures over the Y_a subset.

Marpu et al. (2010) proposed a simple way to analyse segmentation results based on five different criteria:

- Percentage of the area of the biggest overlapping object after excluding the extra area;
- Percentage of lost area;
- Percentage of extra area;
- Number of reference objects that lost more than 25% of its area, and;
- Number of reference objects that gained more than 25% of its area.

For this study, we evaluated each of these five criteria as separated indices:

$$\%BigObj = \frac{area(x_i \cap y_{j\max})}{area(x_i)}, y_{j\max} \in Y_a \quad (6)$$

$$\%LstArea = \frac{area(x_i) - area(x_i \cap y_j)}{area(x_i)}, y_j \in Y_a \quad (7)$$

$$\%ExtArea = \frac{area(y_j) - area(x_i \cap y_j)}{area(x_i)}, y_j \in Y_a \quad (8)$$

%BigObj, *%LstArea* and *%ExtArea* are in [0,1], where *%BigObj* = 100% defines a good segmentation, where the biggest sub-object match the reference object exactly, and, *%LstArea* and *%ExtArea* with 0% being ideal.

For the third and fourth criteria, we simply computed the number of reference objects which had values greater than 25% for the measures described in Eq. (7) and (8). These criteria were used as a penalty factor for the global score (described in the following section). This factor was calculated using the formula:

$$pf_j = N_j * \frac{1}{10} \quad (9)$$

Where pf_j is the penalty factor for the scale parameter j and N_j is the number of objects that gained or lost more than 25% of its area in the scale parameter j.

We decided to combine the third and fourth criteria into a penalty factor (*pf*) since the reference objects that gained or lost 25% are strongly deformed and this scale parameter might not be suitable to effectively represent the objects from that land cover class.

With the exception of the *Relative Area*, which was evaluated on the Y subset, all the goodness measures used in this study were evaluated on the Y_a subset.

2.3.3. Metrics similarity

In this work, a correlation coefficient was used to represent the relationship between the goodness measures. This method simply examined when there is a tendency for two measures to increase or decrease together, called positive correlation, or, for one to increase as the other decreases and vice versa, called negative correlation. The Pearson correlation coefficient is conventionally defined between -1 and +1, where -1 represents strong evidence of negative correlation and; 1 represents strong evidence of positive correlation. Values near 0 tend to occur when there is little or no correlation between the two variables.

The Pearson rank correlation coefficient (r) can be calculated as follows:

$$r = \frac{1}{n-1} * \sum_{i=1}^{n} \left(\frac{x_i - \overline{X}}{S_x} \right) \left(\frac{y_i - \overline{Y}}{S_y} \right) \tag{10}$$

Where r is the Pearson rank correlation coefficient considering the α value of 0.05; n is the sample size; x_i is the value for the variable x; X is the mean value for the variable x; S_x is the standard deviation for the variable x; y_i is the value for the variable y; Y is the mean value for the variable y and; S_y is the standard deviation for the variable y.

In this context, a r value were calculated for each possible pair of goodness measures used in this study in order to verify if these measures are correlated. Two measures with strong correlation values mean that just one of them can be used to effectively evaluate the segmentation.

2.3.4. Identifying the optimal image segmentation scale

To evaluate the segmentation generated at each scale described in the Section 2.2, a score for each measure described in the previous section were calculated. The scores were based on a single-class approach and on a multi-class approach. In the first case, we quantified the quality based on the mean values for the measures considering each class separately. In the second case, the multi-class approach used the mean value for the measures from all the reference objects.

The optimal image segmentation scale relative to the single and multi-class approach was defined as the scale that, after considering each score, maximized the final global score.

For the purpose of describing the score and global score we used, shall us consider $K = \{k_i: i = 1…n\}$, as the set of n goodness measures used in this study. The score ranged from 0 to 10. Thus, each measure had a coefficient (a):

$$a = \frac{\max(k_i) - \min(k_i)}{10}, k_i \in K \quad (11)$$

Where, $\max(k_i)$ is the maximum value of the i measure among the 27 scale parameter combinations, and; $\min(k_i)$ is the minimum value. The coefficient a represents the value that each measure must increase or decrease in their values to get one point from the score. For example, a goodness measure k_i has 0 as the ideal value. In this case, its minimum value $min(k_i)$ gets the highest score (10.0). The next score (9.0) will be given to the $\min(k_i) + a$ value. Then, the next point (8.0) will be given to the $min(k_i) + 2*a$, and so forth. The same approach was used to the measures that have 1 as the ideal value. This method

will ensure that each goodness measure will have a minimum and a maximum score taking into consideration the distribution and amplitude of its values.

The global score can be calculated as follows:

$$GS_j = \sum_{i=1}^{n} S_i - \left(pf_j * \sum_{i=1}^{n} S_i \right), \quad (12)$$

Where GS_j is the global score for scale parameter j; S_i is the score for the measure i, and pf_j is the penalty factor for the scale parameter j.

As most goodness measures give an indication of under-segmentation and over-segmentation, their S value is equally weighted. The *%BigObj* is the only measure with double-weighted S value (with the highest score as 20). This measure represents how much the segmentation matches the reference object. This measure must be taken under consideration since the higher values represent a perfect segmentation, which is desired. A stricter evaluation can be carried out by changing the weights of the measures to verify their influence on the global score.

2.3.5. Visual inspection of the segmentation results

After selecting an optimal image segmentation scale value for each class, the image objects produced by these parameters were compared to the test objects (shown in Figure 3). The quality of the segmentation depends not only on the reference objects, but how well these test objects are represented; otherwise we can assume that the potential segmentation parameter value is only suitable for these specifics reference objects and may not be correctly judged as the best parameter to represent a specific land cover class.

For the evaluation, we based on a qualitative visual inspection of the test objects. We intended, primarily, to identify under-segmented test objects. As mentioned, over-segmented features are more likely to be rebuilt than an under-segmented feature. Thus, an under-segmented feature is not desired as it may not represent the real object and it can strongly affect the overall accuracy of the classification.

3. Results and discussion

3.1. Optimal image segmentation scale

The Global Score (*GS*) values for the selected classes as well as the individual goodness values for each land cover class are summarized in Table 1. In this analysis, we focused on selecting the scale parameter (among the 27 used in this study) which produced the highest *GS* according to each goodness measures.

Comparison of *GS* values for the single-class approach and for the multi-class approach showed the segmentation evaluation process yielded a G*S* ranging from 50 to 59. A brief analysis of Table 1 shows that each land cover class obtained a different scale parameter: 300A for Bareland, 750A for Eucalyptus, 400C for Grassland, 150B for Forest remnants, 100C for Pasture and 400A when considering all reference objects together. This result confirms the fact of a single-scale approach may not be appropriate to represent the entire scene. For example, we found the combination 750A was the most suitable parameter to represent the class *Eucalyptus*. However, if we consider this parameter in a single-scale segmentation, all the other classes will be strongly under-segmented. Liu and Xia (2010) found that classification accuracy decreased substantially when over or under-segmentation occurred. In fact, this

issue is more evident in under-segmentation because under-segmented objects contain more than one land cover class. On the other hand, if we consider the 100C, which is the most suitable parameter for *Pasture*, some classes will be over-segmented.

A stricter evaluation of Table 1 shows that none of the goodness measure used in this study had the highest scores for all the selected land cover classes. This is evident when considering the measure *%BigObj*. Despite the lower values - and consequently lower scores - for *Vegetation* and *Pasture*, these classes showed the highest *GS* values. In fact, this is due the non-participation of *pf* on their *GS* values, making them the highest *GS*.

Table 1. Selected optimal segmentation parameters values according to its highest global score values.

	Bareland	Eucalyptus	Grassland	Vegetation	Pasture	All Classes
QR	0.03257	0.00215	0.01985	0.03533	0.01976	0.05758
Score	7	10	8	8	9	0
RA	0.22700	0.20785	0.20316	0.29545	0.53707	0.20073
Score	5	2	4	6	10	3
OverSeg	0.02364	0.11847	0.02978	0.06821	0.07540	0.02712
Score	4	0	8	9	3	8
UnderSeg	0.03257	0.00215	0.02620	0.03533	0.01976	0.05758
Score	7	10	5	8	9	10
RMS	0.03259	0.08381	0.02847	0.06479	0.05558	0.07339
Score	9	0	8	8	8	4
% Big Obj	59.92%	84.41%	95.64%	44.35%	32.24%	79.41%
Score	12	18	20	6	4	18
%Lst Area	5.69%	10.76%	4.68%	10.36%	7.18%	8.54%
Score	6	0	8	6	7	6

%Ext Area	3.33%	0.16%	2.60%	3.54%	1.87%	6.46%
Score	7	10	6	8	9	10
N	1	0	2	0	0	3
Total Score	**57**	**50**	**67**	**59**	**59**	**59**
pf	10%	0%	20%	0%	0%	15%
Global Score	**51.3**	**50**	**53.6**	**59**	**59**	**50.15**
Selected Scale	**300A**	**750A**	**400C**	**150B**	**100C**	**400A**

Our results indicate that the proposed procedure of the parameter selection is possible. However, this process is still subject to some expert judgment, since a goodness measure or set of measures must be chosen and will influence the global score. A similar procedure was proposed by Costa et al. (2008) and Happ, Feitosa and Street (2012) where they have used an automatic method based on genetic algorithms to automatically adjust the segmentation parameters to a given set of reference objects. Despite of the robustness of their method, it is still subject to some expert judgment regarding the selection of the parameters to be tested, as well as the manually delineated objects.

In addition, we have used measures for both under and over-segmentation problems, and the weights assigned to each measure seem to influence in the global score and, consequently, the ultimate selection. Also, the choice of training objects influences the final selection. Different observers will likely choose different objects and manually segment them differently. However, this must be considered an advantage of this approach: the best segmentation results can be achieved relative to the set of objects which is considered most important to each analyst.

Finally, we strongly feel that this procedure will help to objectively choose segmentation results.

3.2. Visual assessment of segmentation results

For the purpose of evaluating the segmentation produced by the selected segmentation parameter values, a visual assessment of the test objects was performed. Based on visual assessments and interpretation of the test objects, all the scale parameters selected by the proposed procedure were able to depict very well these objects. Our results showed good correspondence between the segmentation results and most of the test objects. However, we observed that three test objects were strongly under-segmented: the Grassland test object D and the Eucalyptus test objects F and H (Figure 5). This is due to the fact that these classes showed the highest values for the scale parameter, 400 and 750, respectively. Also, a brief analysis of the objects in the Figure 3 shows that these objects are close to other spectrally similar features. Therefore, the set of parameters selected for the *Grassland* includes a proportion of 0.5/0.5 (C) for color/shape where the segmentation was performed equally considering the spectral features and the shape of the object.

Despite their well-defined boundaries, these factors may have led the under-segmentation of these objects. On the other hand, the over-segmented test objects (from J to O) may not represent a problem in a further post-segmentation analysis (e.g. classification) as the sub-objects are contained within the borders of the test object and present the same spectral characteristics. It is essential to be able to determine whether inaccuracy in the classification process is due to a poor classifier or a poor segmentation, or even both.

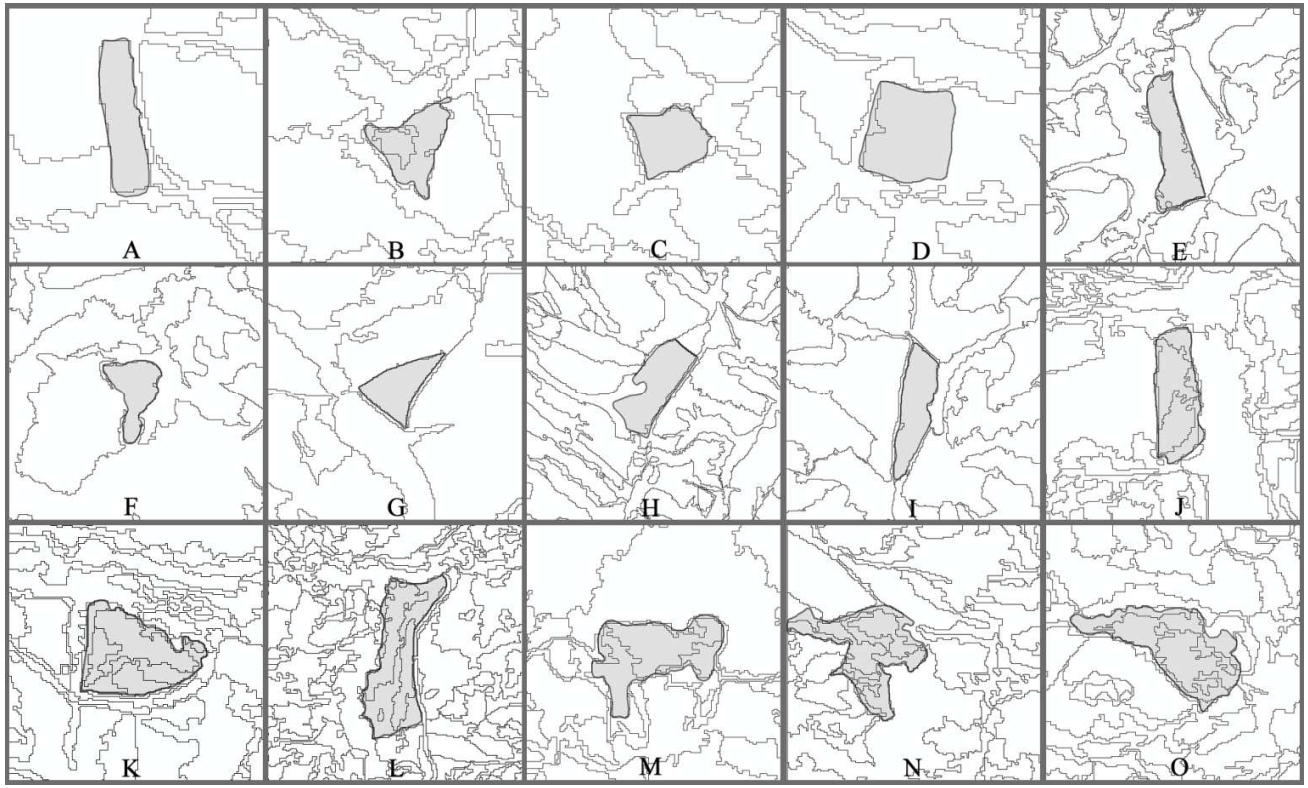

Figure 5. Representation of the manually delineated test objects with the segmentation results for 'Bareland' (A,B and C), 'Eucalyptus'(D, E and F), 'Grassland' (G, H and I), 'Forest remnants' (J, K and L) and 'Pasture' (M, N and O).

3.1. Metrics similarity

In this study, the Pearson correlation coefficient was used to represent the relationship between the goodness measures. We calculated the *r* coefficient for each class separately as well as considering all objects together. The results are summarized in the Tables 2 to 7. We established critical value of 0.80, which means a high correlation between the metrics and in all tables we highlighted the *r* coefficients above this value.

Table 2. Pearson correlation coefficient (*r*) – *Bareland*

	•QR	•RA	•OS	•US	•RMS	•%BG	•%LP	•%EP
•QR	1.00							
•RA	-0.32	1.00						
•OS	-0.43	0.54	1.00					
•US	**1.00**	-0.33	-0.42	1.00				
•RMS	0.36	0.29	0.60	0.38	1.00			
•%BG	**0.85**	-0.54	-0.25	**0.87**	0.42	1.00		
•%LP	-0.10	0.48	**0.94**	-0.08	**0.81**	0.05	1.00	
•%EP	**0.99**	-0.36	-0.54	**0.99**	0.28	**0.82**	-0.22	1.00

Table 3. Pearson correlation coefficient (*r*) – *Eucalyptus*

	•QR	•RA	•OS	•US	•RMS	•%BG	•%LP	•%EP
•QR	1.00							
•RA	-0.11	1.00						
•OS	-0.03	0.47	1.00					
•US	**1.00**	-0.11	-0.03	1.00				
•RMS	0.45	0.31	**0.84**	0.45	1.00			
•%BG	0.70	-0.56	0.10	0.70	0.45	1.00		
•%LP	0.57	0.35	0.72	0.57	**0.91**	0.47	1.00	
•%EP	**1.00**	-0.14	-0.05	**1.00**	0.45	0.71	0.56	1.00

Table 4. Pearson correlation coefficient (*r*) – *Grassland*

	•QR	•RA	•OS	•US	•RMS	•%BG	•%LP	•%EP
•QR	1.00							
•RA	0.45	1.00						
•OS	0.55	0.62	1.00					
•US	**1.00**	0.45	0.55	1.00				
•RMS	0.63	0.61	**0.99**	0.63	1.00			
•%BG	0.39	0.08	0.50	0.39	0.52	1.00		
•%LP	0.68	0.63	**0.98**	0.68	**0.99**	0.52	1.00	
•%EP	**0.99**	0.41	0.49	**0.99**	0.59	0.39	0.64	1.00

Table 5. Pearson correlation coefficient (*r*) – *Eucalyptus*

	•QR	•RA	•OS	•US	•RMS	•%BG	•%LP	•%EP
•QR	1.00							
•RA	-0.08	1.00						
•OS	-0.56	0.64	1.00					
•US	**1.00**	-0.08	-0.56	1.00				
•RMS	0.50	0.51	0.38	0.50	1.00			
•%BG	**0.92**	-0.06	-0.46	**0.92**	0.51	1.00		
•%LP	-0.17	**0.85**	0.79	-0.17	0.49	-0.11	1.00	
•%EP	**1.00**	-0.13	-0.61	**1.00**	0.46	**0.91**	-0.24	1.00

Table 6. Pearson correlation coefficient (*r*) – *Forest remnants*

	•QR	•RA	•OS	•US	•RMS	•%BG	•%LP	•%EP
•QR	1.00							
•RA	-0.29	1.00						
•OS	-0.47	0.45	1.00					
•US	**1.00**	-0.29	-0.47	1.00				
•RMS	0.63	0.07	0.35	0.63	1.00			
•%BG	0.71	-0.73	-0.34	0.71	0.45	1.00		
•%LP	0.46	0.05	0.51	0.46	**0.95**	0.39	1.00	
•%EP	**1.00**	-0.31	-0.48	**1.00**	0.63	0.71	0.46	1.00

Table 7. Pearson correlation coefficient (*r*) – *All classes*

	•QR	•RA	•OS	•US	•RMS	•%BG	•%LP	•%EP
•QR	1.00							
•RA	-0.16	1.00						
•OS	-0.30	**0.86**	1.00					
•US	**1.00**	-0.16	-0.30	1.00				
•RMS	0.54	0.60	0.60	0.54	1.00			
•%BG	**0.92**	-0.40	-0.46	**0.92**	0.36	1.00		
•%LP	0.14	**0.82**	**0.88**	0.14	**0.81**	-0.05	1.00	
•%EP	**0.99**	-0.24	-0.38	**0.99**	0.48	**0.93**	0.04	1.00

As shown in the Tables 2 – 7, most of the metrics are highly correlated. Feitosa et al. (2010) tested the Kendal and the Spearman rank correlations to express the similarity between the metrics. They have found that most of the metrics were highly correlated.

A stricter analysis of our results shows that some metrics presented high values for the *r* coefficient in all cases such as QR and US; QR and %EP, and US and %EP. It was also possible to verify that the correlation coefficients were 1.0 in most of the cases, which means that these metrics are, technically, the same. However, these three metrics were proposed by three different studies. In our study, these metrics were completely redundant which led us to conclude that only one would be sufficient to evaluate the segmentation and, also, this redundancy might have caused an unnecessary increase of the Global Score. As seen in the Eq. 12, the higher the value of *S*, the greater the impact of the penalty factor *fp* in the Global Score. Consequently, this redundancy may have indirectly misled the selection of the scale parameter.

Hence, a stricter evaluation of this procedure may be carried out by eliminating the redundant measures and evaluating the impact in the Global score (*GS*).

4. Conclusions

In this study, we have presented a scale parameter selection procedure based on segmentation goodness measures for selecting the appropriate image segmentation parameter values from a set of potential combinations. Until now, no general approach for selecting parameter exists. We concluded that these measures are not only useful for the selection of segmentation parameters from a pool of potential combinations, but also have utility in reporting the overall accuracy of segmentation, based on reference objects. The advantage of our approach is the selection of a segmentation parameter not based on subjectivity such as expert opinion or visual interpretation. We could also reinforce that a single-scale is not suitable to represent the entire scene.

In a future work, we intend to use this procedure for evaluating different land-cover classes. Additionally, we intend to select new goodness measures and increase the number of reference objects as well as carry out a previous exploratory analysis in order to eliminate the redundant measures.

References

BENZ, U.C., HOFMANN, P., WILLHAUCH, G., LINGERFELDER, I. and HEYNEN, M., 2004, Multi-resolution, object-oriented fuzzy analysis of remote sensing data for GIS-ready information. *ISPRS Journal of Photogrammetry and Remote Sensing*, **58**, pp. 239–258.

BLASCHKE, T., 2010, Object based image analysis for remote sensing. *ISPRS Journal of Photogrammetry and Remote Sensing*, **65**, pp. 2–16.

CARDOSO, J.S. and CORTE-REAL, L., 2005, Toward a generic evaluation of image segmentation. *IEEE Transactions on Image Processing*, **14**, pp. 1773–1782.

CHABRIER, S., EMILE, B., ROSENBERGER, C. and LAURENT, H., 2006, Unsupervised Performance Evaluation of Image Segmentation. *EURASIP Journal on Advances in Signal Processing*, **2006**, pp. 1–13.

CLINTON, N., HOLT, A., SCARBOROUGH, J., YAN, L. and GONG, P., 2010, Accuracy Assessment Measures for Object-based Image Segmentation Goodness. *Photogrammetric Engineering & Remote Sensing*, **76**, pp. 289–299.

COSTA, G.A.O.P., FEITOSA, R.Q., CAZES, T.B. and FEIJÓ, B. 2008. Genetic Adaptation of Segmentation Parameters. In: T. Blaschke, S. Lang & G. J. Hay (eds.): Object-Based Image Analysis – Spatial Concepts for Knowledge-Driven Remote Sensing Applications, Lecture Notes in Geoinformation and Cartography. Springer-Verlag, Berlin, 679-695.

ESPINDOLA, G.M., CAMARA, G., REIS, I.A., BINS, L.S. and MONTEIRO, A.M., 2006, Parameter selection for region growing image segmentation algorithms using spatial autocorrelation. *International Journal of Remote Sensing*, **27**, pp. 3035–3040.

FEITOSA, R. Q., FERREIRA, R. S., ALMEIDA, C. M., CAMARGO, F. F., COSTA, G. A. O. P., 2010. Similarity Metrics for Genetic Adaptation of Segmentation Parameters In: 3rd International Conference on Geographic Object-Based Image Analysis (GEOBIA 2010), 2010, Ghent. 3rd International Conference on Geographic Object-Based Image Analysis. Enshede: ITC, 2010. v.XXXVII.

GALINDO-LEAL, C. and CÂMARA, I.G., 2003, Atlantic Forest hotspots status: an overview In: *The Atlantic Forest of South America: biodiversity status, threats, and outlook.* C. Galindo-Leal, and I.G. Câmara, I.G. (Eds), pp. 3–11. (Washington, D.C: Island Press).

GAVET, Y. and PINOLI, J.-C., 2011, A Geometric Dissimilarity Criterion Between Jordan Spatial Mosaics. Theoretical Aspects and Application

to Segmentation Evaluation. *Journal of Mathematical Imaging and Vision*, **42**, pp. 25–49.

JIANG, X., MARTI, C., IRNIGER, C. and BUNKE, H., 2006, Distance Measures for Image Segmentation Evaluation. *EURASIP Journal on Advances in Signal Processing*, **2006**, pp. 1–11.

KIM, M., MADDEN, M. and WARNER, T., 2008. Object-Based Image Analysis. In Thomas Blaschke, S. Lang, & G. J. Hay, eds. ObjectBased Image Analysis Spatial concepts for knowledgedriven remote sensing applications T Blaschke S Lang and GJ Hay editors SpringerVerlag Berlin In press Kim M. Berlin, Heidelberg: Springer Berlin Heidelberg, pp. 823–870.

LIU, D. and XIA, F., 2010, Assessing object-based classification: advantages and limitations. *Remote Sensing Letters*, **1**, pp. 187–194.

LUCIEER, A. and STEIN, A., 2002, Existential uncertainty of spatial objects segmented from satellite sensor imagery. *IEEE Transactions on Geoscience and Remote Sensing*, **40**, pp. 2518–2521.

MARPU, P.R., NEUBERT, M., HEROLD, H. and NIEMEYER, I., 2010, Enhanced evaluation of image segmentation results. *Journal of Spatial Science*, **55**, pp. 55–68.

MÖLLER, M., LYMBURNER, L. and VOLK, M., 2007, The comparison index: A tool for assessing the accuracy of image segmentation. *International Journal of Applied Earth Observation and Geoinformation*, **9**, pp. 311–321.

NEUBERT, M. and MEINEL, G., 2003, Evaluation of segmentation programs for high resolution remote sensing applications. In: *Joint ISPRS/EARSeL Workshop "High Resolution Mapping from Space 2003*".

ROMÁN-ROLDÁN, R., GÓMEZ-LOPERA, J.F., ATAE-ALLAH, C., MARTÍNEZ-AROZA, J. and LUQUE-ESCAMILLA, P.L., 2001, A

measure of quality for evaluating methods of segmentation and edge detection. *Pattern Recognition*, **34**, pp. 969–980.

SCHIEWE, J., 2002, Segmentation of high-resolution remotely sensed data - Concepts, Applications and Problems. *In Joint ISPRS Commission IV Symposium: Geospatial Theory, Processing and Applications*. pp. 9–12.

WEIDNER, U., 2008, Contribution to the assessment of segmentation quality for remote sensing applications. *In Proceedings of the 21st Congress for the International Society for Photogrammetry and Remote Sensing*. pp. 479–484.

YANG, L., ALBREGTSEN, F., LONNESTAD, T. and GROTTUM, P., 1995, A supervised approach to the evaluation of image segmentation methods. *In V Hlavac & R Sara, eds. Proceedings of 6th International Conference: Computer Analysis of Images and Patterns, Prague, Czech Republic*. pp. 759–765.

ZHANG, H., FRITTS, J.E. and GOLDMAN, S.A., 2008, Image segmentation evaluation: A survey of unsupervised methods. *Computer Vision and Image Understanding*, **110**, pp. 260–280.

ZHANG, X., XIAO, P. and FENG, X., 2012, An unsupervised evaluation method for remotely sensed imagery segmentation. *IEEE Geoscience and Remote Sensing Letters*, **9**, pp.156–160.

ZHANG, Y.J., 1996. A survey on evaluation methods for image segmentation. *Pattern Recognition*, **29**, pp. 1335–1346.

ZOU, K.H. et al., 2004. Statistical validation of image segmentation quality based on a spatial overlap index1. *Academic Radiology*, **11**, pp. 178–189.

CHAPER 3

(Prepared according to International Journal of Remote Sensing guidelines)

OBJECT-BASED CLASSIFICATION WITH SELECTED MACHINE LEARNING ALGORITHMS FOR THE CLASSIFICATION OF VEGETATED AREAS USING HIGH-RESOLUTION RAPIDEYE IMAGERY

C.H.R. de Sousa[a], L.M.T. de Carvalho[a] and K.O. Niemann[b]

Department of Forest Sciences, Federal University of Lavras, Lavras, Brazil

Department of Geography, University of Victoria, Victoria, British Columbia, Canada

[a]Universidade Federal de Lavras, Departamento de Ciências Florestais, Campus Universitário, Caixa Postal 3037, CEP 37200-000, Lavras, MG – Brasil

[b]University of Victoria, Department of Geography, Social Sciences & Mathematics Bldg, Rm B203, 3800 Finnerty Road, Victoria, BC, Canada V8P 5C2

Corresponding author. E-mail: celiohelder@gmail.com

Abstract: An object-based image analysis approach was used for classifying land-cover classes over a vegetated landscape using three supervised machine learning algorithms: Decision Tree (DT), Random Forest (RF), and the Support Vector Machine (SVM). The classification data was a 5m spatial resolution RapidEye image. Classification results provided by the machine learning algorithms were compared in order to evaluate the applicability in the classification of landscapes with high diversity of environmental settings. In terms of overall accuracy, the RF out-performed both DT and SVM with 85.05%. The difference between DT and SVM overall accuracy was 1.18%. A

visual inspection of the maps was also carried out. We observed the RF map, in general, depicted more accurately all the land-cover classes in the region than the other maps produced by DT and SVM algorithms.
Keywords: object-based, decision tree, random forest, support vector machine

1. Introduction

The use of remotely sensed images for mapping and monitoring land cover had fundamental importance in recent decades, in particular, due the development of new techniques and computer programs that enhanced the analysis and manipulation of these digital products. Notable advances are being made in land cover mapping due the technological advancement of the recent and upcoming sensors. These advances rely mostly in the increasing the spatial resolution and in the introduction of additional bands in multi-spectral sensors.

RapidEye represents a constellation of 5 multispectral high-resolution sensors. These satellites are equally spaced around a sun-synchronous orbit and have a spatial resolution of 5 meters (resampled). Recent studies in land cover mapping suggest that pixel-based approaches have disadvantages for such high resolution imagery. One alternative to the pixel-based approach is the framework known as GEOBIA – Geographic Object-Based Image Analysis (Hay and Castilla 2008). Previous studies have proved its advantages over the well-known pixel-based approach (Belaid et al. 1992; Herrera et al. 2004; Yu et al. 2006; Myint et al. 2011). The basic role of this new approach is to merge the adjacent pixels into spectrally homogeneous objects and lead the classification process as the objects being the minimum unit of analysis. Object-level characteristics including shape, size, texture and context within neighbourhoods or hierarchies can all be incorporated into classification decision models. While these additional descriptors can provide improved class or feature

discrimination, incorporating this new information can increase the complexity of the image analysis process.

Over the last years, machine learning algorithms have shown great potential to deal with a high number of predictors from the object-based approach as well as to improve the accuracy and reliability of remote sensing image classification. Several studies have tested a variety of machine learning algorithms in both classification approaches: pixel-based and object-based. In the context of the pixel-based approach, studies such as Huang et al. (2002) compared the accuracies from pixel-based classification produced using four different classification algorithms: support vector machines, decision trees, a neural network classifier, and the maximum likelihood classifier (MLC). Their results showed that the accuracy of the Support Vector Machine classifier outperformed the other three classification algorithms. Pal (2005) compared the accuracies of Support Vector Machines and Random Forests (Breiman 2001) using Landsat Enhanced Thematic Mapper (ETM+) in a pixel-based classification. Their results showed that both algorithms performed equally well. Gislason, Benediktsson and Sveinsson (2006) compared a Random Forest approach to a variety of decision tree-like algorithms using pixel-based classification of Landsat MSS data. They found that the selected tree-based algorithms tested performed similarly, but that the Random Forest algorithm outperformed the standard implementation of the Decision tree proposed by Breiman (2001). Chan and Paelinckx (2008) used Random Forest and Adaboost for the classification of ecotopes using airborne hyperspectral imagery. Their results suggested that both algorithms showed no significant difference in the overall accuracy. Otukei and Blaschke (2010) compared the Maximum Likelihood classifier, Support Vector Machine, and Decision Trees algorithms in a pixel-based approach for land-cover change detection, and found Decision Trees performed better than the others. Laliberte et al. (2006) used an object-

based approach on Quickbird imagery to compare the Nearest Neighbour classifier with Decision Tree algorithms. Their study found that Decisions Trees produced better overall classification accuracies than the Nearest Neighbour classifier. Stumpf and Kerle (2011) used the object-based approach on Quickbird, IKONOS, Geoeye-1, aerial photographs data for mapping landslides. They used the Random Forest classifier and they found accuracies between 73% and 87%.

Therefore, comparisons between pixel-based and object-based image analysis using machine learning algorithms have also been led (Yan et al. 2006; Platt and Rapoza 2008; Myint et al. 2011; Duro, Franklin and Dubé 2012). According to these comparisons, object-based approach produced better overall accuracies and outperformed the pixel-based approach. In general, many comparisons were conducted using a relatively simple classifier, like Nearest Neighbour, for the object-based classifications.

Considering the above comparisons and taking advantage of recent advances in object-based image analysis (OBIA) and machine learning algorithms, this study aims to examine the object-based approach in conducting classifications of a vegetated area in RapidEye data with a selection of machine learning algorithms: Decisions trees, Random Forest and Support Vector Machine.

2. Methods

2.1. Data and study area

A high-resolution RapidEye image data from the southern region of Minas Gerais, Brazil, is used (Figure 1). This data has a 5,0 m spatial resolution with five channels: blue (0,44 – 0,51 μm), green (0,52 – 0,59 μm), red (0,6, –

0,68 μm), red edge (0,69 – 0,73 μm) and near infra-red (0,76 – 0,85 μm) and a radiometric resolution of 12 bit. This data set was acquired at standard processing level (orthorectified) by Minas Gerais state government in June, 2010.

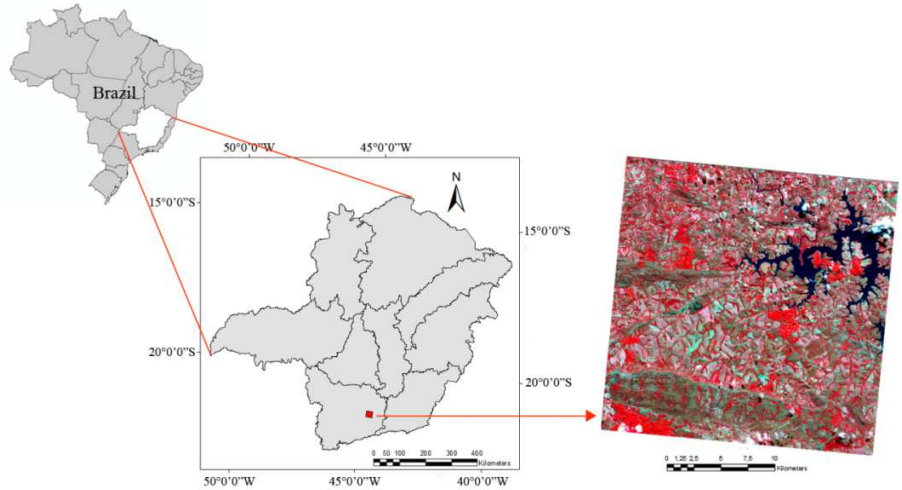

Figure 1. Study area located in Minas Gerais, Brazil.

This image has an area of 77 x 77 km over the municipalities of São Vicente de Minas, Minduri, Cruzília, Luminárias and Carrancas. The area is part of the Rio Grande basin, in the micro region of Lavras and its vegetation is characterized as an encounter between Brazilian savanna and Brazilian Atlantic Rainforest, forming rocky fields and gallery forests. The Brazilian Atlantic Rainforest is one of the most important biome in the country and originally covered approximately 1 million square kilometers within 17 states, representing 16% of the country (Galindo-Leal and Câmara 2003). However, the Brazilian Atlantic Rainforest has been under degradation since the colonial period due the agricultural cycles and the expansion of cultivated areas. Hence, it occupies approximately 98000 square kilometers, or 8% of its original area and is still under strong anthropogenic pressure resulting in a high risk of extinction.

The land-cover in the study area basically includes: grassland, forest remnants, pasture areas, eucalyptus and open water. We intentionally selected this image by its wide variety of environmental settings due these land-cover classes which have homogeneous internal properties and most of the classes are separated by well-defined boundaries. Therefore, this area is under constant degradation due the agricultural activities and its mapping is an important source of information about how this degradation has been occurring over the years.

2.2. Image segmentation and feature selection

Image segmentation represents the first step in object-based image analysis. Many segmentation algorithms have been developed in recent years, all of them aiming a homogeneous image segments. The multi-resolution image segmentation (MRS) implemented in eCognition Developer® software is a frequently used algorithm in Earth sciences (Blaschke 2010). The MRS algorithm uses a "bottom-up" region neighboring objects based on a set of user-defined parameters such as scale, color/shape, and smoothness/compactness defining a "stopping threshold". Additional information regarding the segmentation algorithm can be found in Benz et al. (2004).

The initial RapidEye image analysis included segmenting the image at a relatively fine scale (400) using eCognition Developer® version 8.0. The MRS offers the possibility to assign different weights to the spectral bands of the image. In this study, all the spectral bands (blue, green, red, red edge and near infrared) were equally weighted. The value of color/shape used was 0.1 and compactness/smoothness was 0.5. We intentionally chose this combination of parameters according to a previous analysis in which 27 scale+color/shape combinations were used to generate different scenarios for segmentation evaluation. Our results showed that the 400 scale was the most suitable for all

the classes. This parameter sufficiently delineated small features of the scene such as small forest remnants, small areas of pasture and agriculture.

Following the image segmentation process, object features were selected for use in the object-based classification. Selecting object features can be a subjective process based on the user knowledge or like in Yu et al. (2006), where the authors used a CART approach to select the features to use in the classification. In this study we focused on our prior knowledge of the area to select the object features. These features are listed in Table 1.

Table 1. Object-features used in the classification process.

Object features	
Spectral information	Spectral bands mean values*
	Band Ratios (NDVI and SAVI)
	Brightness
	Max difference between pixel values
Texture $GLCM_{alldirections}$	Mean*
	Homogeneity*
	Standard deviation*
Geometry	Area
	Roundness
	Compacity
	Boundarie index/Shape
	Length/Width

* Object features were calculated for each spectral band

In addition to the features found in the software, the NDVI index (Rouse 1973) (Eq.1) and SAVI (Huete 1988) (Eq. 2) were also calculated to widen the feature input for the classification process.

The global NDVI and SAVI can be calculated as follows:

$$NDVI = \frac{NIR - RED}{NIR + RED} \quad (1)$$

$$SAVI = \frac{NIR - RED}{(NIR + RED + L)} * (1 + L) \quad (2)$$

Where *NIR* is the reflectance in the near infrared band; *RED* is the reflectance in the red band; and *L* represents the amount or cover of green vegetation. In regions highly vegetated, L=0; and in areas with no green vegetation, L=1. In this study we used L=0.5.

The total number of object features available to the object-based classification is 38, considering that some features (marked with '*') were calculated for all spectral bands, as seen in Table 1. The unmarked features were calculates considering individual image objects.

2.3. Sampling data

In this study a visual interpretation of the RapidEye imagery as well as the data from Mapeamento da Flora Nativa e dos Reflorestamentos de Minas Gerais (Scolforo, Carvalho and Oliveira 2008) were used to select the ground reference data. Eight broad land-cover classes were selected for this study: bareland, grassland, eucalyptus, forest remnants, water bodies, pasture areas, clouds and shadow. For the purpose of selecting samples to use in the machine learning algorithms, a random sampling approach was used. At first, 1100 objects were randomly selected within the scene. Image objects produced using the MRS algorithm can vary in size and may contain more than one land-cover class. Thus, these objects were carefully examined using visual interpretation as well as the data from Mapeamento da Flora Nativa e dos Reflorestamentos de Minas Gerais (SCOLFORO, CARVALHO and OLIVEIRA 2008) to assess the

homogeneity of the land cover types in the image objects and to ensure all the classes were proportionally represented. Objects with more than one land cover type were not used, leaving a total of 1005 objects. Therefore, each object was classified as one of the eight classes. These objects were then split into two smaller sets of samples using random proportional sampling, referred as *training* and *test* samples. Approximately 70% of the samples (684) were used to train the machine learning algorithms and 30% of the samples (321) were used for accuracy assessment purposes. For setting the parameters and testing the models used by the machine learning algorithms, we used a repeated k-fold cross-validation based on the training data set only. We did not use the test sample in this evaluation.

2.4. Accuracy Assessment

Two measures for assessing the accuracy for thematic maps were used in this study: i) overall accuracy and ii) the Kappa coefficient. The overall accuracy is easily interpretable as the proportion of correctly classified samples, which gives a general overview of the classification results. For each classification, a confusion matrix was presented. A confusion matrix is a two-dimension contingency table, formed by reference data and thematic data, where the reference data is presented as the columns of the matrix and the thematic data, is presented as rows in the matrix. The diagonal entries represent the correctly classified samples and the off-diagonal entries represent the misclassified samples. From this matrix, accuracy measures were calculated such as overall accuracy, user's and producer's accuracy and Kappa coefficient. All these indices were calculated using the *test* samples.

2.5. Setting up the machine learning algorithms parameters

The construction, tuning and accuracy assessment of the models were performed using R version 2.15, a multiplatform, open-source language and software for statistical computing (R Development Core Team 2010). A quick review of the available literature shows that R has been intensively used for classification of remote sensing data using machine learning algorithms (Gislason, Benediktsson and Sveinsson 2004; Lawrence and Sheley 2006; Sesnie et al. 2008; Stumpf and Kerle 2011; Duro, Franklin and Dublé 2012).

For creating the machine learning algorithms used in this study, we used several packages within the R environment:

- For the Decision Tree models (DTs), we used the recursive partitioning 'rpart' package created by Therneau and Ripley (2010) based on the CART algorithm developed by Breiman et al. (1984);
- For the construction of the Random Forest models (RFs) we used the 'randomForest' package (Liaw and Wiener 2002). For further information about RF algorithms and its codes, we encourage readers to refer to Breiman (2001), and;
- For the Support Vector Machine (SVMs) we used the 'kernlab' package (Karatzoglou et al. 2004).

Each of the algorithms used in this study has parameters that need to be defined by the user. To avoid the subjectivity of randomly choosing these parameters, we examined a pool of potentials parameters using all three machine learning algorithms.

For each model, a confusion matrix was generated using the original training samples. We considered the optimum parameters those that achieved the highest value of overall accuracy in this process. This approach will ensure that only models with higher accuracy will be used in the classification process.

2.5.1.Decision tree based models

A decision tree classifier is a non-parametric classifier that does not require any a priori statistical assumptions to be made regarding the distribution of data. The tree is composed of a root node (formed from all of the data), a set of internal nodes (splits), and a set of terminal nodes (leaves). The DT classification is a procedure which recursively partitions a data set into smaller subdivisions on the basis of a set of tests defined at each split (or node) in the tree. The decision of each node is on the form:

$\sum_{i=1}^{n} a_i x_i \leq c_k$; for multivariate decision tree, or $x_i > c_k$ for univariate trees,

where x_i is the ith input feature, c_k is a suitably chosen threshold and a_i is a vector of linear discriminate coefficient (Brodley and Utgoff 1992). The DTs are known to produce results of higher accuracies in comparison to traditional approaches such as the 'box' and 'minimum distance to means'. In addition, they handle nonlinear relations between features and classes, allow for missing values, and are capable of handling both numeric and categorical inputs.

For the DTs, the parameter 'maximum depth' is a user-defined parameter and it represents the maximum depth of any single node of the trees. In general, higher values of 'maximum depth' will generated more complex trees whereas low values will produce less complex trees. In both cases, it may affect the overall accuracy. For the purposes of choosing the value of 'maximum depth' which provides a model with higher overall accuracy, we tested eight values of 'maximum depth': 4, 6, 8, 10, 12, 14, 16, 18 and 20. The parameter

with the highest value of overall accuracy was considered the optimum parameter to be used in the model.

2.5.2. Random Forest based models

Random Forest is a general term for ensemble methods using tree-type classifier {DT(x, θ_k), m = 1,…,}, where the θ_k are independent identically distributed random vectors and x is an input pattern. The RF classification algorithm is described in detail in Brieman (2001). Briefly, the RF is an ensemble of classification trees, where each tree contributes with a single vote for the assignment of the most frequent class to the input data. Different from DTs, which use the best predictive variables at the splits, RF uses a random subset of predictive variables in order to reduce the generalization error.

In addition, the RF ensemble classifier uses a bagging or boot-strap aggregating, making the trees to grow from different training data subsets to increases the diversity of the trees. Bagging is a technique used for training data creation by randomly resampling the original dataset with replacement. This technique will ensure that each tree contains a certain proportion of the training dataset. On the other hand, the samples which are not present in the training subset are included as part of another subset called “out-of-bag” (OOB). For every tree of the ensemble, a different OOB subset is formed from the non-selected elements. These OOB elements, which are not considered for the training of the tree, can be classified by the tree to evaluate performance of the ensemble.

The RF presents many desirable properties, such as high accuracy, robustness against over-fitting the training data, and integrated measures of variable importance

For the RFs based models, two user-defined parameters exist: the number of trees used in the model (*ntrees*), which represents the number of trees to grow in the 'forest', and the number of variables tested in each split of the trees (m_{try}). For these two parameters, we tested a combination of three values of *ntrees* (500, 1000 and 1500) and eight values of m_{try} (1, 4, 8, 10, 15, 20, 30 and 38) comprising 24 different models. As seen in the previous section, we selected the one of the 24 pairs of parameters which provided the highest overall accuracy value.

2.5.3. Support Vector Machine based models

The support vector machines (SVMs) are a set of related learning algorithms used for classification and regression that uses machine learning theory to maximize predictive accuracy while automatically avoiding over-fit to the data. Like the Decision Trees classifiers, SVMs are also non-parametric classifiers. Its first formulation was originally proposed by Vapnik (1979). Readers are encouraged to refer to Vapnik (1999), for further discussion and details on SVMs and Mountrakis, Im and Ogole (2011) for a review on SVMs in remote sensing.

The success of the SVM depends on how well the process is trained. The easiest way to train the SVM is by using linearly separable classes. According to Osuna, Freund and Girosi (1997), if the training data with k number of samples

is represented as $\{X_i, y_i\}$, $i=1,\ldots,k$ where $X \in R^N$ is an N-dimensional space and y

$\in$ {-1, =1} is a class label, then these classes are considered linearly separable if

there exists a vector *W* perpendicular to the linear hyper-plane (which determines the direction of the discriminating plane) and a scalar b showing the offset of the discriminating hyper-plane from the origin. For the two classes, i.e. class 1 represented as -1 class 2 represented as +1, two hyper-planes can be used to discriminate the data points in the respective classes. These can be expressed as:

- $WX_i + b \geq +1$ for all $y = +1$, i.e. a member of class 1
- $WX_i + b \geq +1$ for all $y = -1$, i.e. a member of class 2

The two hyper-planes are selected not only to maximize the distance between the two given classes but also not to include any points between them. The overall goal is to find out in which class the new data points fall. In general, the SVMs are reported to produce results of higher accuracies compared with the traditional approaches, but the outcome depends on: the kernel used, choice of parameters for the chosen kernel, and the method used to generate SVM (Huang et al. 2002).

For the SVMs based models, a Radius Basis Function (RBF) kernel was used. Others kernels were not taken into consideration in this study. In SVMs based models, there are two user defined parameters: “cost” (C) and “sigma” (σ). “Cost” controls the smoothness of the fitted function. It creates a soft margin that permits some misclassifications. Increasing the value of C increases the cost of misclassifying points and forces the creation of a more accurate

model that may not generalize well. In the other hand, increasing “sigma” affects the shape of the hyperplane and may also affect the overall accuracy. In our study, we tested several values of “cost” (C): 0.1, 0.5, 1, 1.5, 2, 4, 6, 8, 10, 30, 60 and 120. The parameter “sigma” (σ) was estimated using the ‘sigest’ function implemented in ‘kernlab’ package. This function allows estimating an appropriate sigma value directly from the data set. Thus, C was the only parameter tested for the SVM models.

3. Results and discussion

3.1. Image segmentation results

In this study a high-resolution RapidEye image was segmented at a single level using a scale parameter of 400. We performed the segmentation using eCognition Developer® version 8.0. A partial view of the segmentation results can be seen in Figure 2.

It is known that a specific set of parameters may produce a good segmentation result when considering a homogeneous scene but this is not valid when a heterogeneous scene is under consideration. Since the landscape mostly consist of different types of environmental settings and varies in size (e.g. trees, rivers, forest remnants, etc.), a single-scale approach might not be appropriate as the features within the scene will be under-segmented (when part of the feature become part of another feature) or over-segmented (when the feature is segmented into smaller objects). Thus, it may affect the final overall accuracy of the classifications.

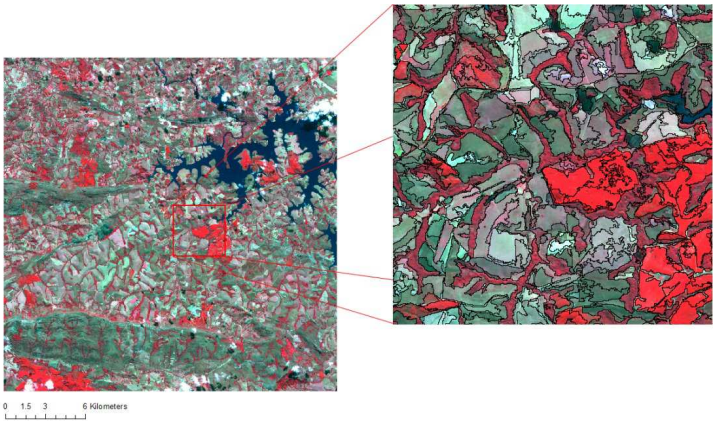

Figure 2. Representation of the segmentation results using a scale parameter of 400. Objects of forest remnants (dark red), eucalyptus (red), grassland (green), pasture area (light pink), water (dark blue), bareland (light blue), clouds (white) and shadow (black) were well delineated.

However, our results suggest that, even considering a single-scale approach, the set of parameters used in the segmentation process was sufficiently adequate to delineate most of the objects within the scene and consequently generate relative high accuracy values for the three classifications. Figure 2 shows an example of delineated objects from all land cover classes used in this study. In general, even small objects of clouds and irregular patches of natural vegetation were well delineated using a single scale approach. The segmentation parameters were chosen according to a previous analysis in which 27 scale+color/shape combinations were used to generate different scenarios for segmentation evaluation. We based our evaluation in goodness measures available in the literature. The results showed that a value of 400 for the scale parameter was the most suitable for all classes of interest.

3.2. Optimized machine learning algorithms parameters

For the Decision tree based models, ‘maximum depth’ values ranging from 4 to 20 were tested. Based on the highest accuracy value (96.05%), the model with ‘maximum depth’ value of 4 was selected to be used in the final classification. In studies such as Friedl and Brodley (1997) a ‘maximum depth’ value of 20% of the size of the tree was selected. In this approach, however, the overall accuracy of the model may not be the highest if we consider they did not tested other levels of maximum depth. In Amoro-Lopéz et al. (2011) a ‘maximum depth’ value was estimated with a 10-fold cross validation procedure. In this case, the tree is pruned based on an optimal scheme that prunes branches offering less improvement to error cost.

For the RF models, an overall accuracy of 97.22% was obtained with a m_{try} value of 4 and a *ntree* value of 500. Breiman and Cutler (2007) suggested the default *ntree* as 500 for Random Forest based classifications since values greater than 500 appeared to have little influence in the overall classification accuracy. In our analysis, the overall accuracy converged to 93.66% when we used 1000 and 1500 as found in Breiman (1996) who suggested that when increasing the number of trees the generalization error always converges. The same number of trees (500) was used in studies such as Lawrence and Sheley (2006), Gislason, Benediktsson and Sveinsson (2004), Stumpf and Kerle 2011 and Duro, Franklin and Dublé 2012.

For the classification using SVMs, the value of σ was estimated using the ‘sigest’ function and it was held constant at 0.01915945. An overall accuracy of 98.68% was achieved using a C value of 6.

3.3. Visual inspection of the thematic maps

The thematic maps produced by the three different algorithms are presented in the Figure 3. The major visual difference between the maps is the

amount of ‘pasture areas’ and ‘bareland’ depicted in the entire scene. We observed that both maps produced by DT and SVM algorithms (Figure 3C and Figure 3D) present less ‘pasture area’ than the map produced by RF, whereas the SVM map depicted a greater amount of ‘bareland’ areas than DT and RF maps. Based on our knowledge of the region, some pasture areas are severely degraded with portions of exposed soil, which might have caused the misclassification of ‘pasture area’ as ‘bareland’ in the SMV map. Therefore, the predominance of ‘bareland’ in the SVM map was also caused by the misclassification of ‘grassland’ as ‘bareland’. In the DT map, some areas of ‘bareland’ were classified into ‘clouds’ due the fact that both classes are spectrally similar, which caused the misclassification. On the other hand, we observed that the depiction of ‘forest remnants’ and ‘eucalyptus’ was relatively consistent in all maps. These classes are similar, considering their spectral features. Although the algorithms differed slightly in the depiction of some vegetated areas, all the three algorithms depicted both classes very well. Likewise, the class ‘water’ was well defined in all maps, although presenting some misclassified patches in the left and lower portions of the DT map.

We carried out a visual inspection of the RapidEye scene and considering our experience in the area, we observed the RF map, in general, depicted more accurately all the land-cover classes in the region (Figure 3B) than the other maps produced by DT and SVM algorithms.

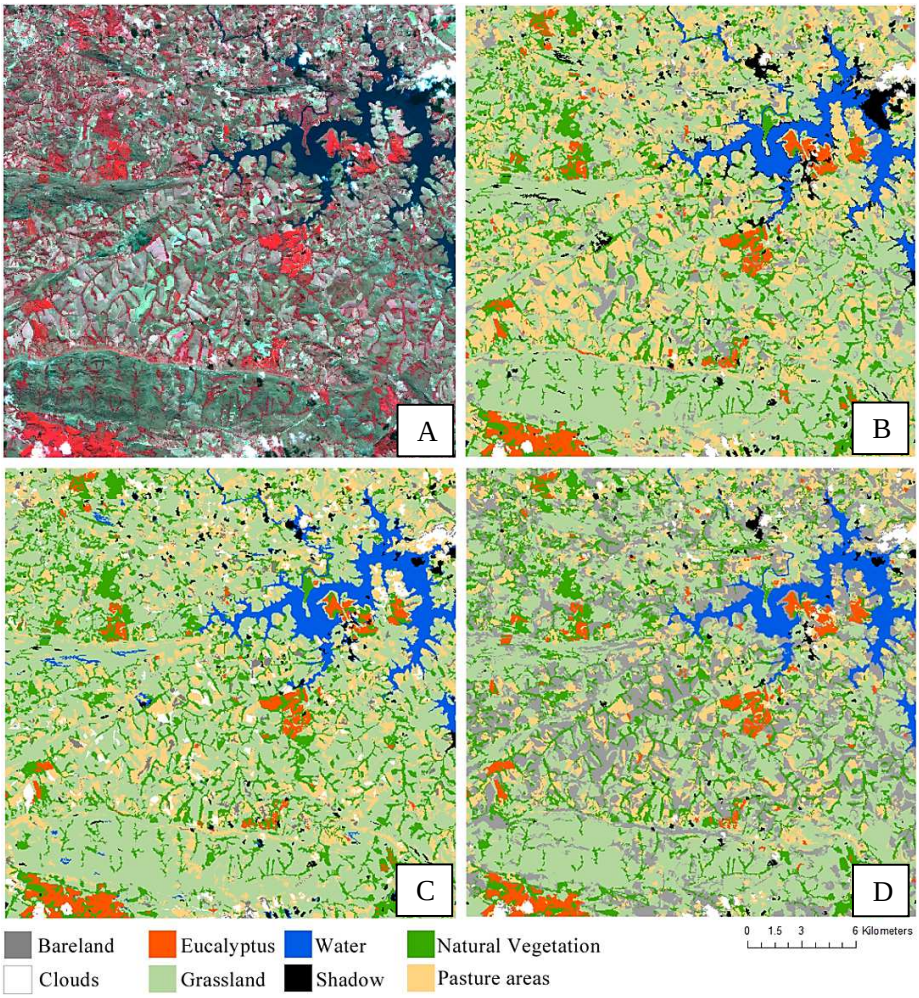

Figure 3. Object-based classifications: A) RapidEye image in false color RGB532; B) Random Forest based classification; C) Decision Tree based classification; D) Support Vector Machine based Classification.

3.4. Accuracy Assessment

An accuracy assessment using 'test samples' (321) was carried out for each classification produced in this study to evaluate the performance of the models. Table 2, 3 and 4 contains the detailed confusion matrices for the RF, DT

and SVM based models, respectively. Overall, user's and producer's accuracy as well as Kappa coefficients were calculated.

Based on the overall accuracies of the confusion matrices, the object-based classification using Random forest obtained an overall accuracy of 85.05% which was higher than 75.70% from Support Vector Machine classification and 71.34% from Decision Tree classification. Their Kappa coefficient values were 0.8312, 0.7218 and 0.6704, respectively. Since its first implementation in Breiman (2001), the Random Forest has been showing its superiority over a variety of other machine learning algorithms in remote sensing studies. For example, Pal (2005) compared RF based models and SVM based models in a pixel-based classification approach and also found an overall accuracy consistently over 80% for the RF classification which was higher than the SVM. Duro, Franklin and Dubé (2012), in a pixel-based approach, also found a higher overall accuracy for the Random forest based classification. However, the Support Vector Machine based model was slightly superior (1,18%) to the Random Forest in the object-based classification.

When comparing the overall accuracy values from DT and SVM models, the SVM model showed a slight improvement (4.36%) over the DT classification.

However, considering a visual inspection of these maps, the DT map showed a reasonably accurate visual depiction of the land-cover classes in this area. Considering its simple implementation, compared to the SVM, and even to RF, the DT model was effective in dealing with such variable land-cover classes.

Table 2. Confusion matrix for the Random Forest based classification

Classification Data	Reference Data									User's Accuracy (%)
	Bareland	Vegetation	Pasture	Meadow	Eucalyptus	Water	Clouds	Shadow	TOTAL	
Bareland	**31**	0	1	0	0	0	4	0	36	86.11
Vegetation	0	**40**	1	0	10	0	0	0	51	78.43
Pasture área	0	0	**34**	0	0	0	0	0	34	100.00
Grassland	0	1	17	**59**	0	0	0	0	77	76.62
Eucalyptus	0	2	3	0	**44**	0	0	0	49	89.80
Water	0	0	0	0	0	**10**	0	0	10	100.00
Clouds	4	0	0	0	0	0	**38**	0	42	90.48
Shadow	0	0	0	0	1	4	0	**17**	22	77.27
TOTAL	35	43	56	59	55	14	42	17	**321**	
Producer's Accuracy (%)	88.57	93.02	60.71	100.00	80.00	71.43	90.48	100.00		
Overall Accuracy (%)	85.05									
Kappa Coeficient	0.8312									

Table 3. Confusion matrix for the Decision Tree based classification

Classification Data	Reference Data									User's Accuracy (%)
	Bareland	Vegetation	Pasture	Meadow	Eucalyptus	Water	Clouds	Shadow	TOTAL	
Bareland	**22**	0	0	0	0	0	9	0	*31*	70.97
Vegetation	0	**40**	1	0	16	0	0	0	*57*	70.18
Pasture área	4	0	**8**	0	0	0	0	0	*12*	66.67
Grassland	0	1	30	**59**	0	0	0	0	*90*	65.56
Eucalyptus	0	2	3	0	**38**	0	0	0	*43*	88.37
Water	0	0	0	0	0	**13**	0	1	*14*	92.86
Clouds	9	0	14	0	0	0	**33**	0	*56*	58.93
Shadow	0	0	0	0	1	1	0	**16**	*18*	88.89
TOTAL	*35*	*43*	*56*	*59*	*55*	*14*	*42*	*17*	***321***	
Producer's Accuracy (%)	62.86	93.02	14.29	100.00	69.09	92.86	78.57	94.12		
Overall Accuracy (%)	71.34									
Kappa Coeficient	0.6704									

Table 4. Confusion matrix for the Support Vector Machine based classification

Classification Data	Reference Data									User's Accuracy (%)
	Bareland	Vegetation	Pasture	Meadow	Eucalyptus	Water	Clouds	Shadow	TOTAL	
Bareland	**31**	0	20	6	0	1	0	1	59	52.54
Vegetation	0	**34**	0	0	12	0	0	0	46	73.91
Pasture área	0	2	**20**	0	2	0	0	0	24	83.33
Grassland	0	7	16	**53**	2	0	0	4	82	64.63
Eucalyptus	0	0	0	0	**39**	0	0	0	39	100.00
Water	0	0	0	0	0	**12**	0	0	12	100.00
Clouds	4	0	0	0	0	0	**42**	0	46	91.30
Shadow	0	0	0	0	0	1	0	**12**	13	92.31
TOTAL	35	43	56	59	55	14	42	17	**321**	
Producer's Accuracy (%)	88.57	79.07	35.71	89.83	70.91	85.71	100.00	70.59		
Overall Accuracy (%)	75.70									
Kappa Coeficient	0.7218									

The next comparison was based on the user's and the producer's accuracies, which measure the commission and omission errors, respectively, for each land-cover class. The commission errors represents the probability that an object classified on the map actually represents that class on the ground. On the other hand, the omission errors refers to the probability of a reference object (referred as test sample in this study) being correctly classified.

Both RF and SVM maps presented two classes with no commission errors: 'Pasture areas' and 'Water' for the RF map and 'Eucalyptus' and 'Water' for the SVM map. For land cover types with distinctive spectral features such as 'water' it is common to have good values of user's accuracy. On the other hand, land cover types with similar spectral features such as 'Forest remnants' and 'Eucalyptus' also had good values for user's accuracy (ranging from 70 to 100%).'Bareland' did not have a good user's accuracy for the SVM map (52.54%) and it was the lowest value for all the classes in the three classifications. As seen in the Figure 2, this map over-represented the class, probably because most of bareland pixels were actually mixed with or around other land cover-classes, which made it difficult to distinguish with an object-based approach. However, RF presented a high user's accuracy for this class (86.11%) and it was clearly more efficient than the others.

In terms of producer's accuracy, the DT and RF maps presented no omission error for the class Grassland (e.g. all test samples for this class were correctly classified), while the SVM map presented high user's and producer's accuracy for the class 'clouds'. Comparing the three algorithms in terms of user's and producer's accuracy, it is clear that each algorithm had its strengths and its weakness in dealing with a specific land cover class.

4. Conclusions

An object-based classification of RapidEye imagery using selected machine learning algorithms was performed. This paper investigated the capability of three machine learning algorithms (Random Forest, Decision Tree and Support Vector Machine) in conducting classifications in a vegetated area. In terms of visual assessments and overall accuracy, the RF based classification over-performed both DT and SVM classifications. Another advantage of the Random Forest classifier is that it requires two relative simple parameters to be set, whereas the SVM, for example, requires complex parameters to be set for its training.

However, considering each class separately, each algorithm had a different performance, which may lead us to conclude that different machine learning algorithms might be used for the classification of different land-cover classes. In a future work, we intend to carry a stricter analysis of these machine learning algorithms in order to select the one which provides the best depiction for a specific land-cover class and combine their results into a new map to enhance the overall accuracy and its reliability.

References

AMORÓS LÓPEZ, J., IZQUIERDO VERDIGUIER, E., GÓMEZ CHOVA, L., MUÑOZ MARÍ, J., RODRÍGUEZ BARREIRO, J.Z., CAMPS VALLS, G. and CALPE MARAVILLA, J., 2011, Land cover classification of VHR airborne images for citrus grove identification. *ISPRS Journal of Photogrammetry and Remote Sensing*, **66**, pp. 115–123.

BENZ, U.C., HOFMANN, P., WILLHAUCK, G., LINGENFELDER, I. and HEYNEN, M., 2004, Multi-resolution, object-oriented fuzzy analysis of

remote sensing data for GIS-ready information. *ISPRS Journal of Photogrammetry and Remote Sensing*, **58**, pp. 239–258.

BELAID, M.A., EDWARDS, G., JATON, A., THOMSON, K.P.B. and BEAULIEU, J.M., 1992, Post-segmentationclassification of images containing small agricultural fields. *Geocarto International*, **3**, pp. 53–60.

BLASCHKE, T., 2010, Object based image analysis for remote sensing. *ISPRS Journal of Photogrammetry and Remote Sensing*, **65**, pp. 2–16.

BREIMAN, L., 1996, Bagging predictors. *Machine Learning*, **24**, pp. 123–140.

BREIMAN, L., 2001, Random Forests. *Machine Learning*, **45**, pp. 1–33.

BREIMAN, L. and CUTLER, A., 2007, Random forests–Classification description: Random forests. Accessed August 15: http://stat-www.berkeley.edu/users/breiman/RandomForests/cc_home.htm

BRODLEY, C.E. and UTGOFF, P.E., 1992, Multivariate versus univariate decision trees. Technical Report 92-8. University of Massachusetts, Amherst, MA, USA

CHAN, J.C.-W. and PAELINCKX, D., 2008, Evaluation of Random Forest and Adaboost tree-based ensemble classification and spectral band selection for ecotope mapping using airborne hyperspectral imagery. *Remote Sensing of Environment*, **112**, pp. 2999–3011.

DURO, D.C., FRANKLIN, S.E. and DUBÉ, M.G., 2012, A comparison of pixel-based and object-based image analysis with selected machine learning algorithms for the classification of agricultural landscapes using SPOT-5 HRG imagery. *Remote Sensing of Environment*, **118**, pp. 259–272.

FRIEDL, M. A. and BRODLEY, C.E., 1997, Decision tree classification of land cover from remotely sensed data. *Remote Sensing of Environment*, **61**, pp. 399–409.

GALINDO-LEAL, C. and CÂMARA, I.G., 2003, Atlantic Forest hotspots status: an overview In: *The Atlantic Forest of South America: biodiversity status, threats, and outlook*. C. Galindo-Leal, and I.G. Câmara, I.G. (Eds), pp. 3–11. (Washington, D.C: Island Press)

GISLASON, P., BENEDIKTSSON, J. and SVEINSSON, J., 2006, Random Forests for land cover classification. *Pattern Recognition Letters*, **27**, pp. 294–300.

GISLASON, P.O., BENEDIKTSSON, J.A. and SVEINSSON, J.R., 2004, Random forest classification of multisource remote sensing and geographic data. *In*: *IEEE International IEEE International IEEE International Geoscience and Remote Sensing Symposium, 2004. IGARSS '04. Proceedings. 2004*. IEEE, pp. 1049–1052.

HAY, G.J. and CASTILLA, G., 2008, Geographic Object-Based Image Analysis (GEOBIA): A new name for a new discipline. In: *Object Based Image Analysis*. Blaschke, T., Lang, S., Hay, G. (Eds.), pp. 75–88 (Berlin, NY: Springer, Heidelberg)

HERRERA, B., KLEIN, C., KOCH, B. and DEES, M., 2004, Automatic classification of trees outside forest using an object-driven approach: An application in a Costa Rican landscape. *Photogrammetrie, Fernerkundung, Geoinformation* , **8**, pp. 111–119.

HUANG, C., DAVIS, L.S. and TOWNSHEND, J.R.G., 2002, An assessment of support vector machines for land cover classification. *International Journal of Remote Sensing*, **23**, pp. 725–749.

HUETE, A.R., 1988. A soil-adjusted vegetation index (SAVI). *Remote Sensing of Environment*, **25**, pp. 295–309.

KARATZOGLOU, A., SMOLA, A., HORNIK, K. and ZEILEIS, A., 2004, kernlab – An S4 Package for Kernel Methods in R. *Journal of Statistical Software*, **11**, pp. 1–20.

LALIBERTE, A.S., RANGO, A., HAVSTAD, K.M., PARIS, J.F., BECK, R.F., MCNEELY, R. and GONZALEZ, A.L., 2004, Object-oriented image analysis for mapping shrub encroachment from 1937 to 2003 in southern New Mexico. *Remote Sensing of Environment*, **93**, pp. 198–210.

LAWRENCE, R.L., WOOD, S.D. and SHELEY, R.L., 2006, Mapping invasive plants using hyperspectral imagery and Breiman Cutler classifications (randomForest). *Remote Sensing of Environment*, **100**, pp. 356–362.

LIAW, A. and WIENER, M., 2002, Classification and regression by randomForest. RNews, **2**, pp. 18–22.

MOUNTRAKIS, G., IM, J. and OGOLE, C., 2011. Support vector machines in remote sensing: A review. *ISPRS Journal of Photogrammetry and Remote Sensing*, ***66***, pp. 247–259.

MYINT, S.W., GOBER, P., BRAZEL, A., GROSSMAN-CLARKE, S. and WENG, Q., 2011, Per-pixel vs. object-based classification of urban land cover extraction using high spatial resolution imagery. *Remote Sensing of Environment*, **115**, pp. 1145–1161.

OSUNA, E., FREUND, R. and GIROSI, F., 1997, Support Vector Machines: Training and Applications, A.I. Memo No. 1602, C.B.C.L. Paper No. 144. Massachusetts Institute of Technology and Artificial Intelligence Laboratory, Massachusetts.

OTUKEI, J.R. and BLASCHKE, T., 2010, Land cover change assessment using decision trees, support vector machines and maximum likelihood classification algorithms. *International Journal of Applied Earth Observation and Geoinformation*, **12**, pp. S27–S31.

PAL, M., 2005, Random forest classifier for remote sensing classification. *International Journal of Remote Sensing*, **26**, pp. 217–222.

PLATT, R.V. and RAPOZA, L., 2008, An Evaluation of an Object-Oriented Paradigm for Land Use/Land Cover Classification. *The Professional Geographer*, **60**, pp. 87–100.

R Development Core Team, 2011, R: A language and environment for statistical computing. R Foundation for Statistical Computing, Vienna, Austria. ISBN 3-900051-07-0, URL http://www.R-project.org/.

ROUSE, J.W., HAAS, R.H., SCHELL, J.A. and DEERING, D.W., 1973, Monitoring vegetation systems in the Great Plains with ETRS. In: *Proceedings of Third ETRS Symposium*, NASA SP353, Washington DC, pp. 309– 317.

SCOLFORO, J.R.S. and CARVALHO, L.M.T., 2008. *Mapeamento e inventário da flora nativa e dos reflorestamentos em Minas Gerais*. UFLA, Lavras, 288p.

STUMPF, A. and KERLE, N., 2011, Object-oriented mapping of landslides using Random Forests. *Remote Sensing of Environment*, **115**, pp. 2564–2577.

VAPNIK, W.N., 1999, An overview of statistical learning theory. *IEEE Transactions of Neural Networks*, **10**, pp. 988–999.

VAPNIK, V., 1979. *Estimation of Dependences Based on Empirical Data*. Nauka, Moscow, pp. 5165–5184, 27 (in Russian) (English translation: Springer Verlag, New York, 1982)

THERNEAU, T. M. and RIPLEY, B. A., 2010, rpart: Recursive Partitioning. Available at: http://CRAN.R-project.org/package=rpart

YAN, G., MAS, J.F., MAATHUIS, B.H.P., XIANGMIN, Z. and VAN DIJK, P.M., 2006, Comparison of pixel-based and object-oriented image classification approaches—a case study in a coal fire area, Wuda, Inner Mongolia, China. *International Journal of Remote Sensing*, **27**, pp. 4039–4055.

YU, Q., GONG, P., CLINTON, N., BIGING, G., KELLY, M. and SCHIROKAUER, D., 2006, Object-based Detailed Vegetation Classification with Airborne High Spatial Resolution Remote Sensing Imagery. *Photogrammetric Engineering & Remote Sensing*, **72**, pp. 799–811.

APPENDIX A – R Tutorials for classification

Decicion Trees

```
Blue: Function
Green: Example of application.

#------------------## DECISION TREE ##--------------#

#------------## DATA ##------------#

## CHANGE DATA DIRECTORY

## LOAD RPART AND FOREIGN PACKAGES (IF INSTALLED)
library(rpart)
library(foreign)

## CREATING DATA OBJECT
object'sname=read.dbf("File_name.dbf")

Ex: data=read.dbf("TRAINING_2.dbf")


#-------## FITTING DECISION TREE MODEL ##-------#

## SETTING THE FIRST PARAMETERS
control=rpart.control(maxdepth=value,cp=value)

Ex: control=rpart.control(maxdepth=30,cp=0.001)

## MODEL
object=rpart(formula~,data=data_frame_with_the_predict
ors, method="class"(for classification),
control=dataframe_with_the_parameters,xval=value)

Ex: dados.dt=rpart(CLASSNAME ~,data=dados[,c(2,3:40)],
method = "class",control=control,xval=10)

## CONFUSION MATRIX
table(groundtruth_samples,predict(decision_tree_object
,type="vector"))

Ex: table(dados$CLASSNAME, predict(dados.dt, type =
"vector"))
```

```
##-----------------CLASSIFICATION-----------------#

## CREATING DATA OBJECT
samples_for_prediction=read.dbf("unclassified_samples_
file_name.dbf")

Ex: predict=read.dbf("UNCLASSIFIED.dbf")
predict.new=predict[,3:40]

## PREDICTING CLASSES
prediction_object_name=predict(decision_tree_object,
newdata=samples_for_prediction, type="class")

Ex: DT=predict(dados.dt,newdata=predict.new,
type="class")

## EXPORTING CLASSES FOR A NEW DATAFRAME
Ex: Class <- data.frame(predict[,1],DT)

## EXPORTING CLASS TO A .DBF FILE
Ex: write.dbf(Class,file='Classes_DT.dbf')
```

Random Forest

```
Blue: Function
Green: Example of application.

#-----------------## RANDOM FOREST ##--------------#

#-----------## DATA ##-----------#

## CHANGE DATA DIRECTORY

## LOAD RANDOMFOREST AND FOREIGN PACKAGES (IF
INSTALLED)
library(randomForest)
library(foreign)

## CREATING DATA OBJECT
object’s_name=read.dbf(“File_name.dbf)
Ex: data=read.dbf("TRAINING.dbf")
```

```
#--------## FITTING RANDOM FOREST MODEL ##--------#

## MODEL
Randomforest_object= randomForest(formula,data=
data_frame_with_the_predictors,ntree=value,mtry=value,
importance=TRUE, na.action=na.omit)

print(Randomforest_object)## for the results and
confusion matrix

Ex: RF <- randomForest(CLASSNAME ~ .,
data=dados[,c(2,3:40)], ntree=500, mtry=8,
importance=TRUE, na.action=na.omit)

## VARIABLES IMPORTANCE
imp <- importance(RF)
print(imp)
varImpPlot(RF)

##----------------CLASSIFICATION-----------------#

## CREATING DATA OBJECT
samples_for_prediction=read.dbf("unclassified_samples_
file_name.dbf")

Ex: predict=read.dbf("UNCLASSIFIED.dbf")
predict.new=predict[,3:40]

## PREDICTING CLASSES
prediction_object_name=predict(Randomfores_object,
samples_for_prediction)

Ex: rf.pred <- predict(dados.rf,predict.new)

## EXPORTING CLASSES FOR A NEW DATAFRAME
Ex: Class <- data.frame(predict[,1],dt.pred)

## EXPORTING CLASS TO A .DBF FILE
Ex: write.dbf(Class,file='Classes_RF.dbf')
```

Support Vector Machine

```
Blue: Function
Green: Example of application.

#----------## SUPPORT VECTOR MACHINE##-------------#

#-----------## DATA ##-----------#

## CHANGE DATA DIRECTORY

## LOAD KERNLAB AND FOREIGN PACKAGES (IF INSTALLED)
library(kernlab)
library(foreign)

## CREATING DATA OBJECT
object’s_name=read.dbf(“File_name.dbf)

Ex: data=read.dbf("TRAINING.dbf")

#-------## FITTING DECISION TREE MODEL ##-------#

## SETTING THE FIRST PARAMETERS

## Optimal Sigma Value For The Kernel Function using
sigest Functino
object=sigest(formula~.,data=data_frame_with_the_predi
ctors)

Ex: srange <- sigest(CLASSNAME~.,data=dados)
s <- srange[2]
rbf <- rbfdot(sigma=s)

## MODEL
SVM_Object=ksvm(formula~.,data=data_frame_with_the_pre
dictors, type"C-bsvc",
kernel=kernel_function,C=value,prob.model=TRUE,cross=k
-fold_crossvalidation)

Ex: SVM <- ksvm(CLASSNAME ~ .,
data=dados[,c(2,3:40)],type="C-
bsvc",kernel=rbf,C=1,prob.model=TRUE, cross=10)
```

```
## CONFUSION MATRIX
table(groundtruth_samples,predict(SVM_object,type="res
ponse"))

Ex: table(dados$CLASSNAME, predict(SVM, type =
"response"))

##-----------------CLASSIFICATION-----------------#

## CREATING DATA OBJECT
samples_for_prediction=read.dbf("unclassified_samples_
file_name.dbf")

Ex: unclassified=read.dbf("UNCLASSIFIED_2.dbf")

## PREDICTING CLASSES
prediction_object_name=predict(SVM_object,
samples_for_prediction)

Ex: Class <- predict(SVM,unclassified[,3:40])

## EXPORTING CLASSES FOR A NEW DATAFRAME
Class2 <- data.frame(predict[,1],Class)
head(out,30)

## EXPORTING CLASSES TO A .DBF FILE
Ex: write.dbf(Class2,file='Classes_SVM.dbf')
```